Extragalactic planetary nebulae as kinematic tracers and distance indicators

Roberto H. Méndez
Institute for Astronomy
University of Hawaii, Honolulu
March 2013

This talk includes work done by:

- Ana M. Teodorescu (Pisa, Italy)
- L. Cliff Johnson (Seattle, USA)
- Hsin-Yi Shih (Honolulu, USA)
- Payel Das (London, U.K.)
- Denise R. Gonçalves (Rio de Janeiro, Brazil)
- Flavio De Lorenzi (Winterthur, Switzerland)
- Ortwin Gerhard, Eric Emsellem
  (Garching near Munich, Germany)

Topics

- Extragalactic PN detection; slitless radial velocities
- VLT + FORS; Subaru + FOCAS; the PN.Spectrograph
- Galaxies observed with FORS and FOCAS
- PN photometry and PNLF distances
- Quasi-Keplerian declines of losvσ; their interpretation
- PNs are good kinematic tracers
- A final test of radial anisotropy?
- Rotation
- Deep spectroscopy of very distant PNs
- Summary of unsolved problems

A typical PN spectrum

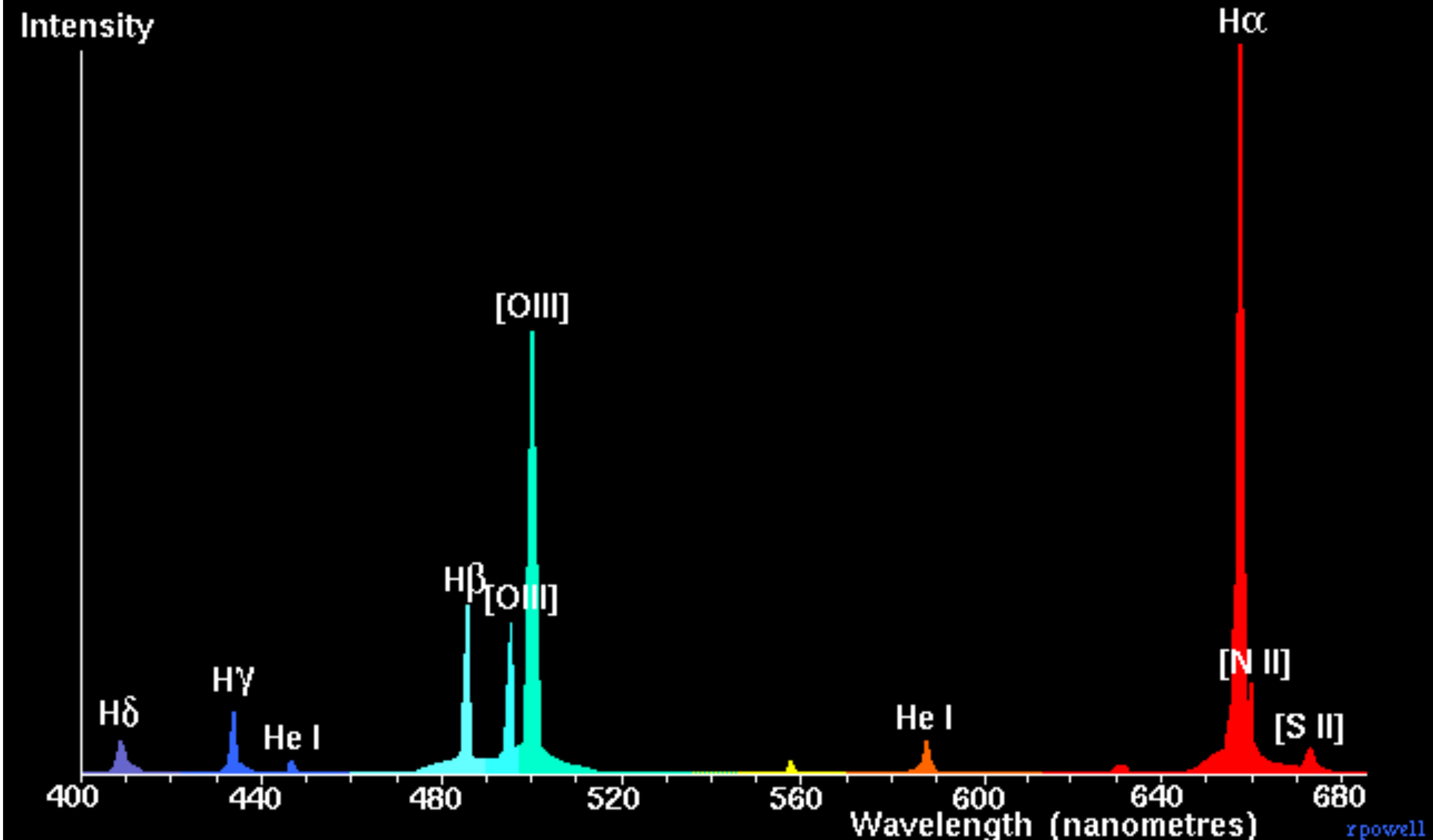

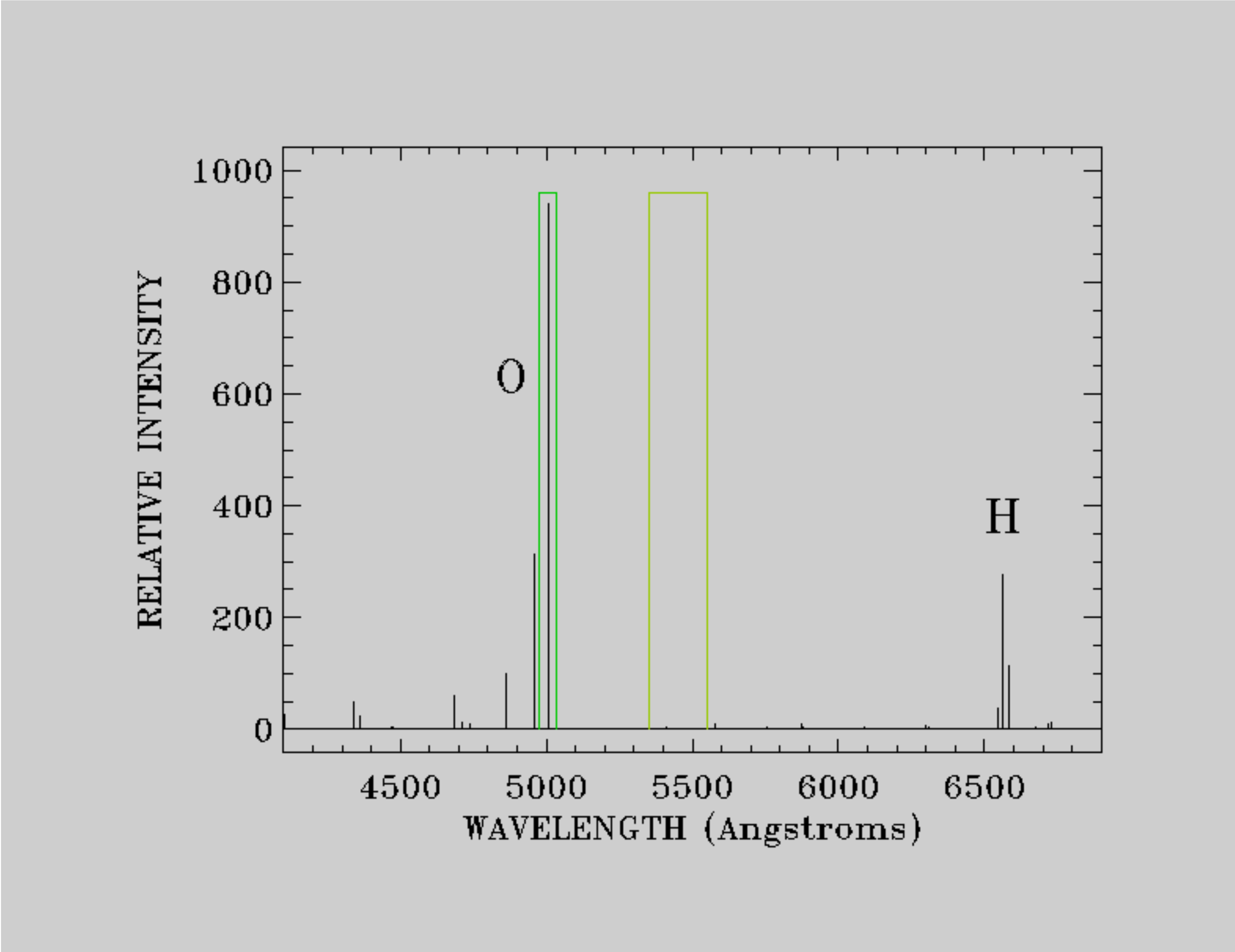

RELATIVE INTENSITY
1000
800
600
400
200
0
O
H
4500
5000
5500
6000
6500
WAVELENGTH (Angstroms)

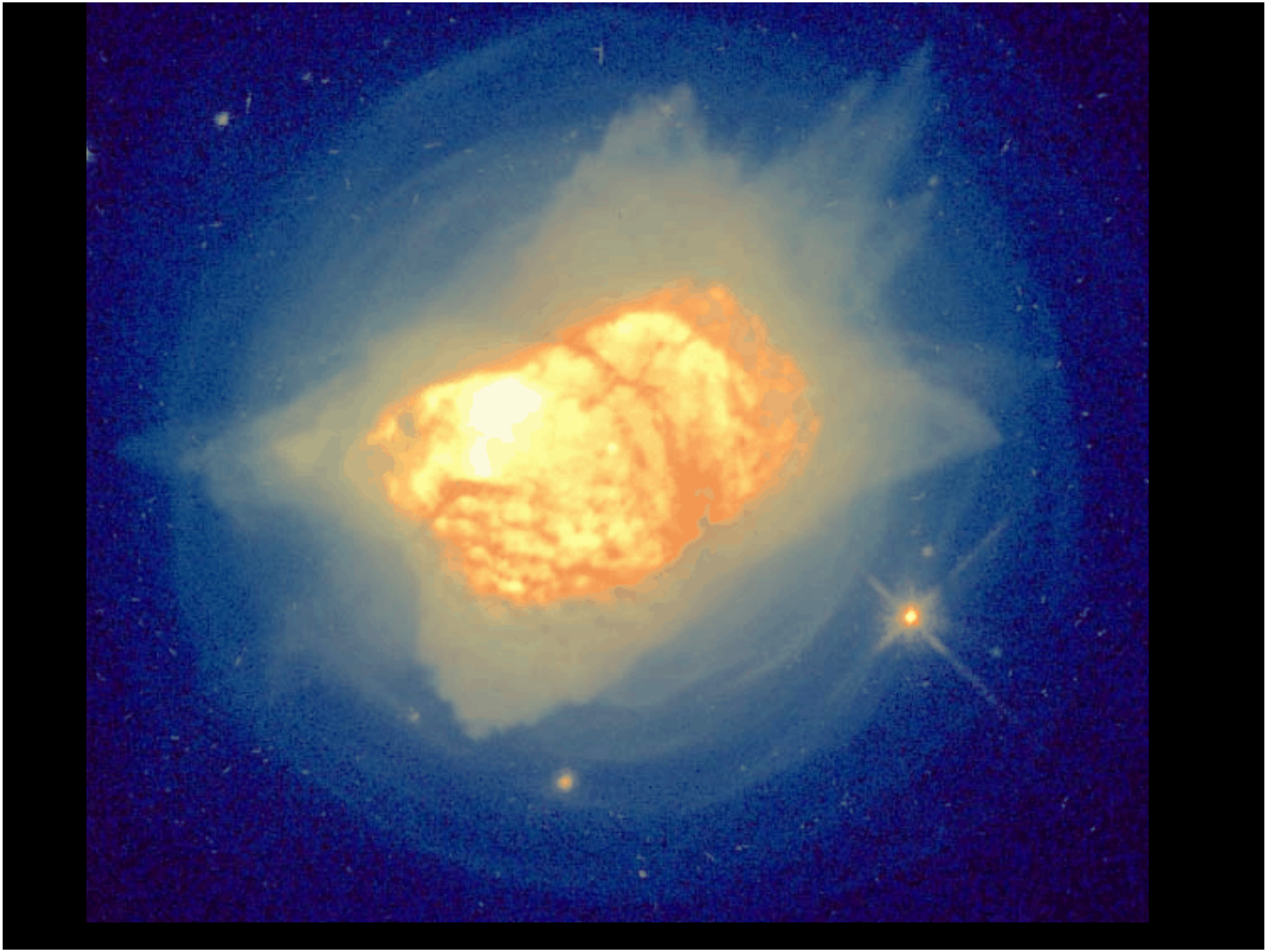

(Subaru + FOCAS) PN search

- The same method was applied earlier with VLT+FORS
- Take offband, onband, onband+grism exposures. The image displacement produced by the insertion of the grism is a function of position and radial velocity of the source. Field of view 6x6 arc min.
- Dispersing element: echelle grism, used in 4^{th} order. We get 0.5 Angstroms/pixel.
- Calibration of grism displacement using a rigid mask with approximately 1000 holes.
- The mask can be illuminated with a comparison lamp, and also with a big local PN, like NGC 7293 (Helix).
- Error in velocities: ~15-20 km/s.

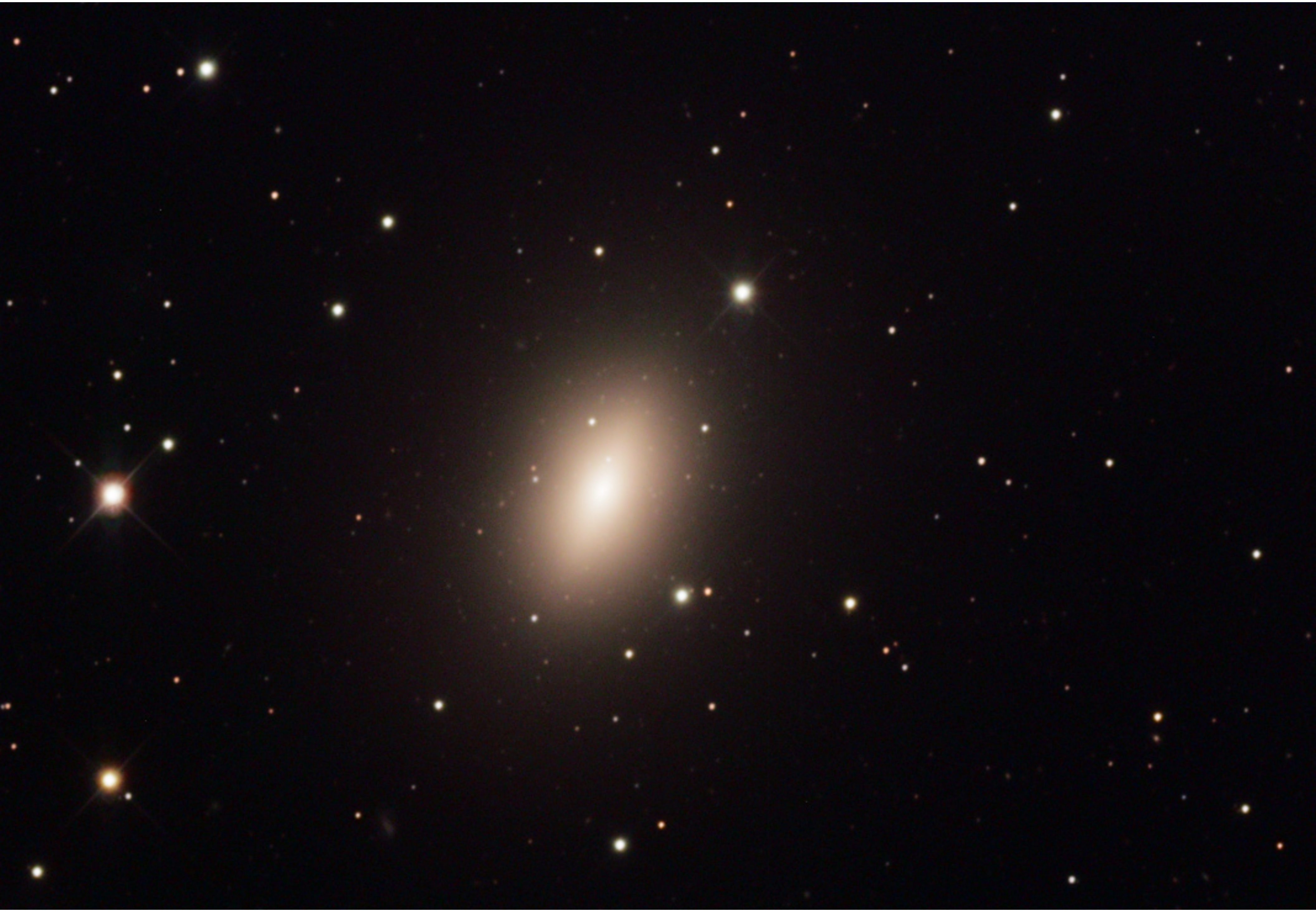

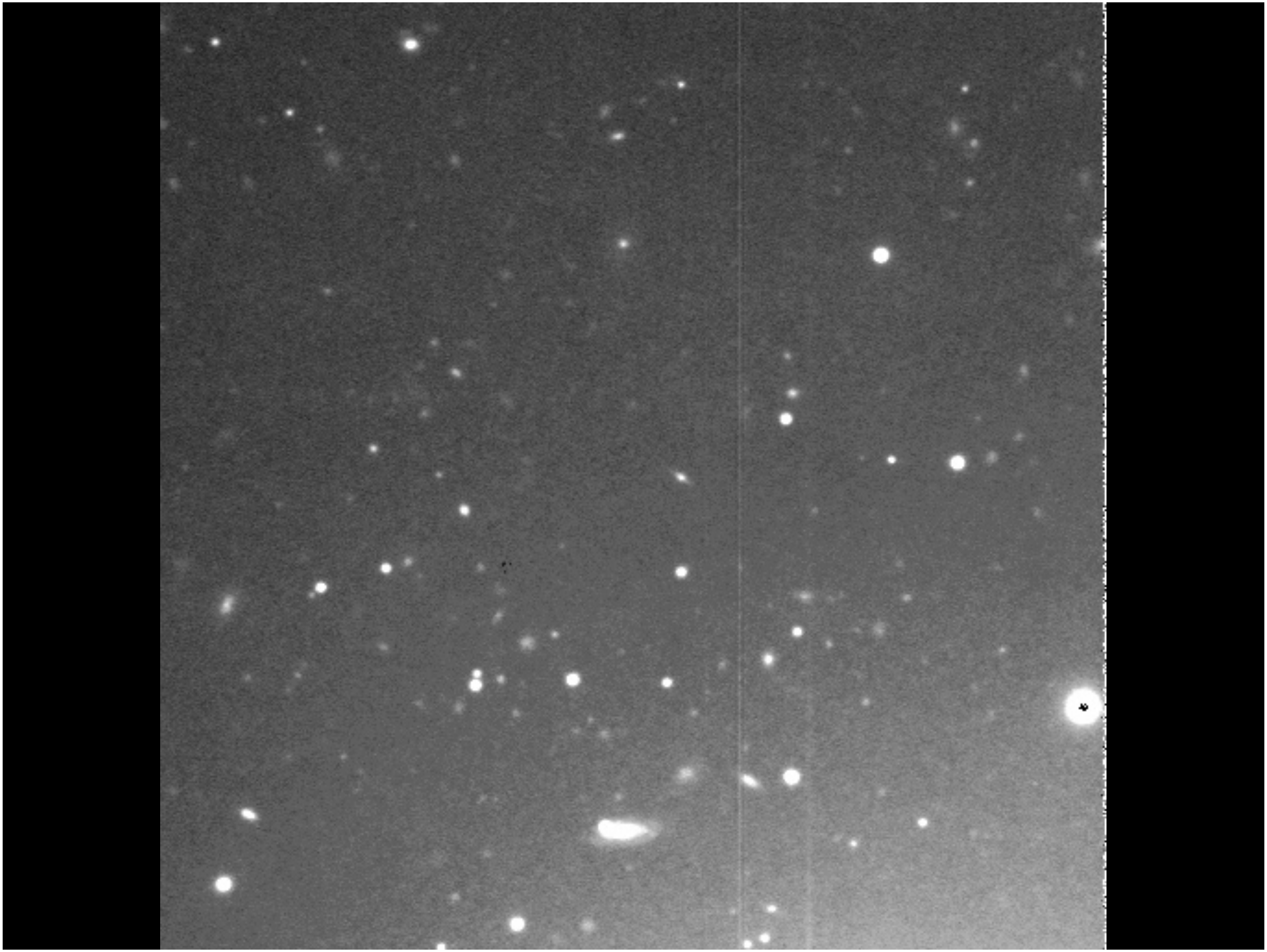

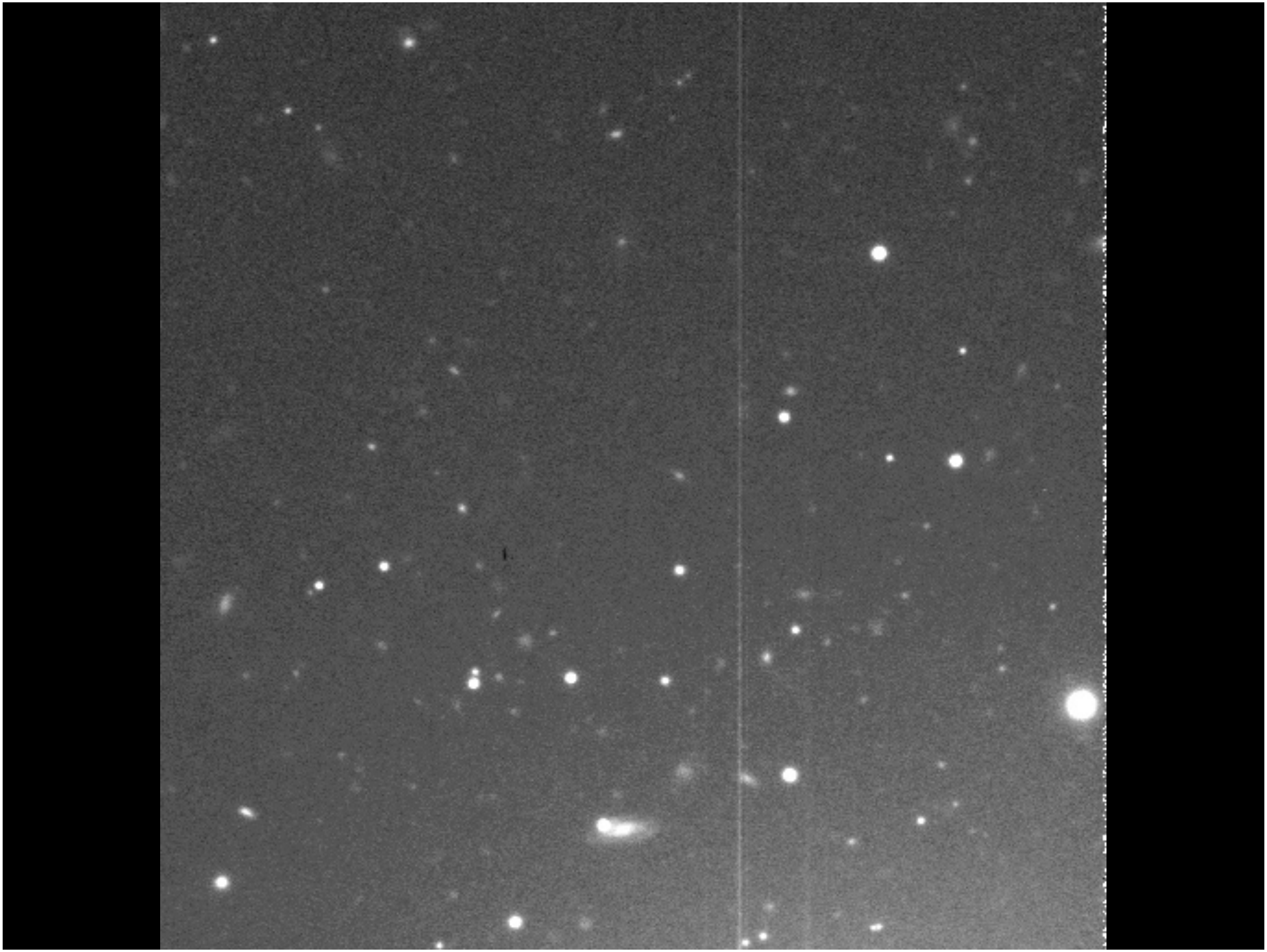

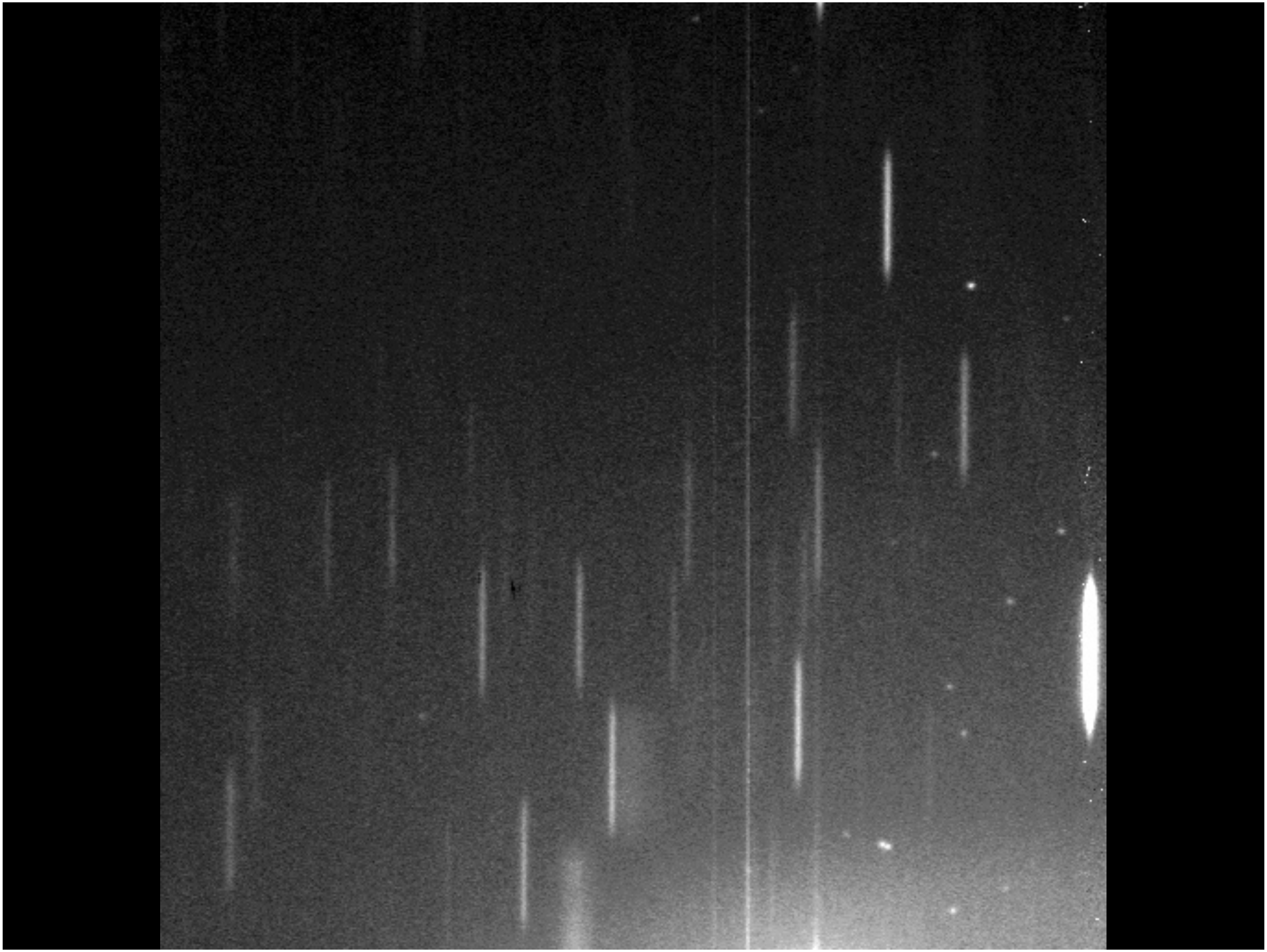

Calibration Fun

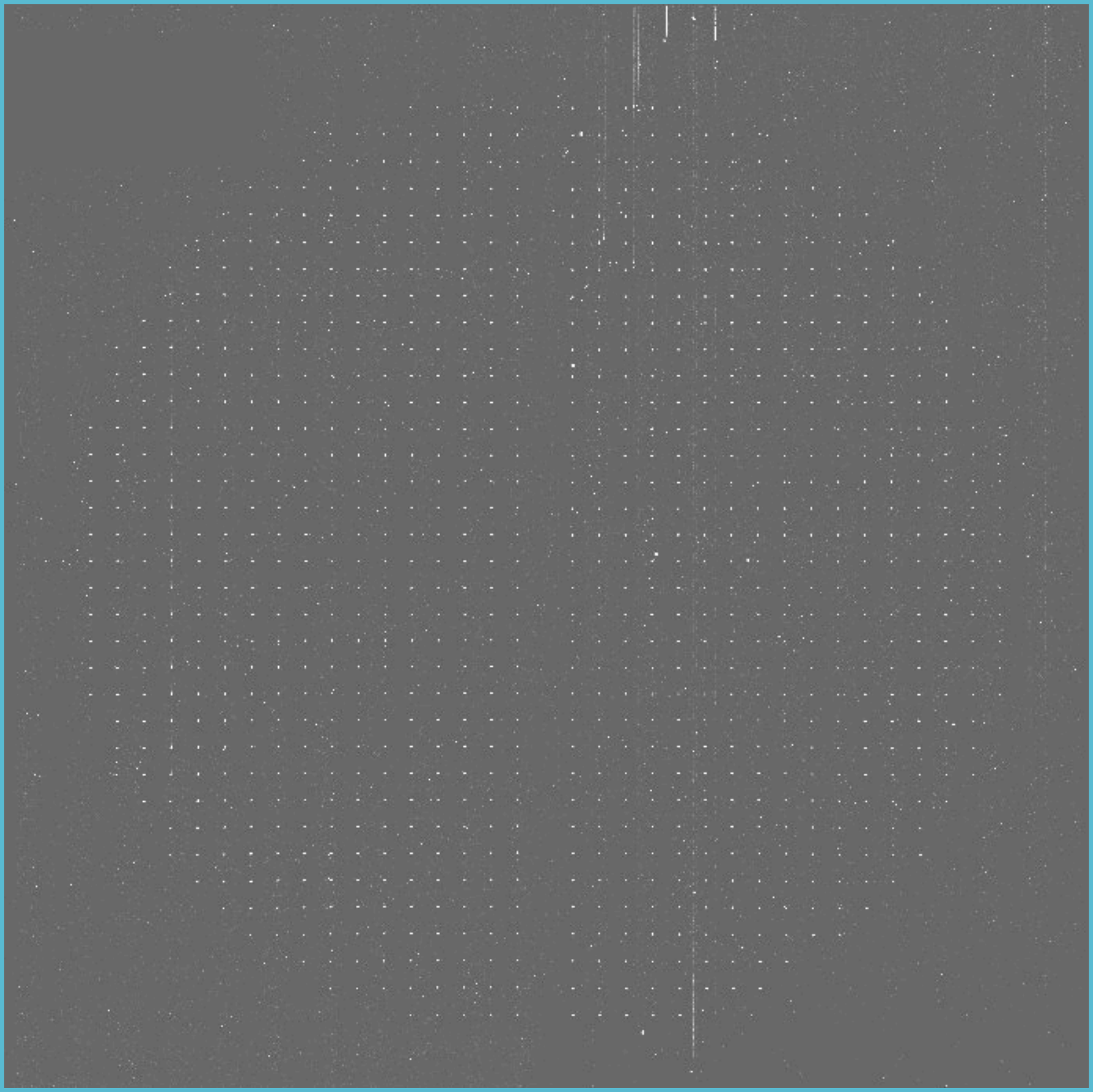

Thorium-Argon Lamp

through an

Engineering Mask

970 points

≈100 pixel spacing

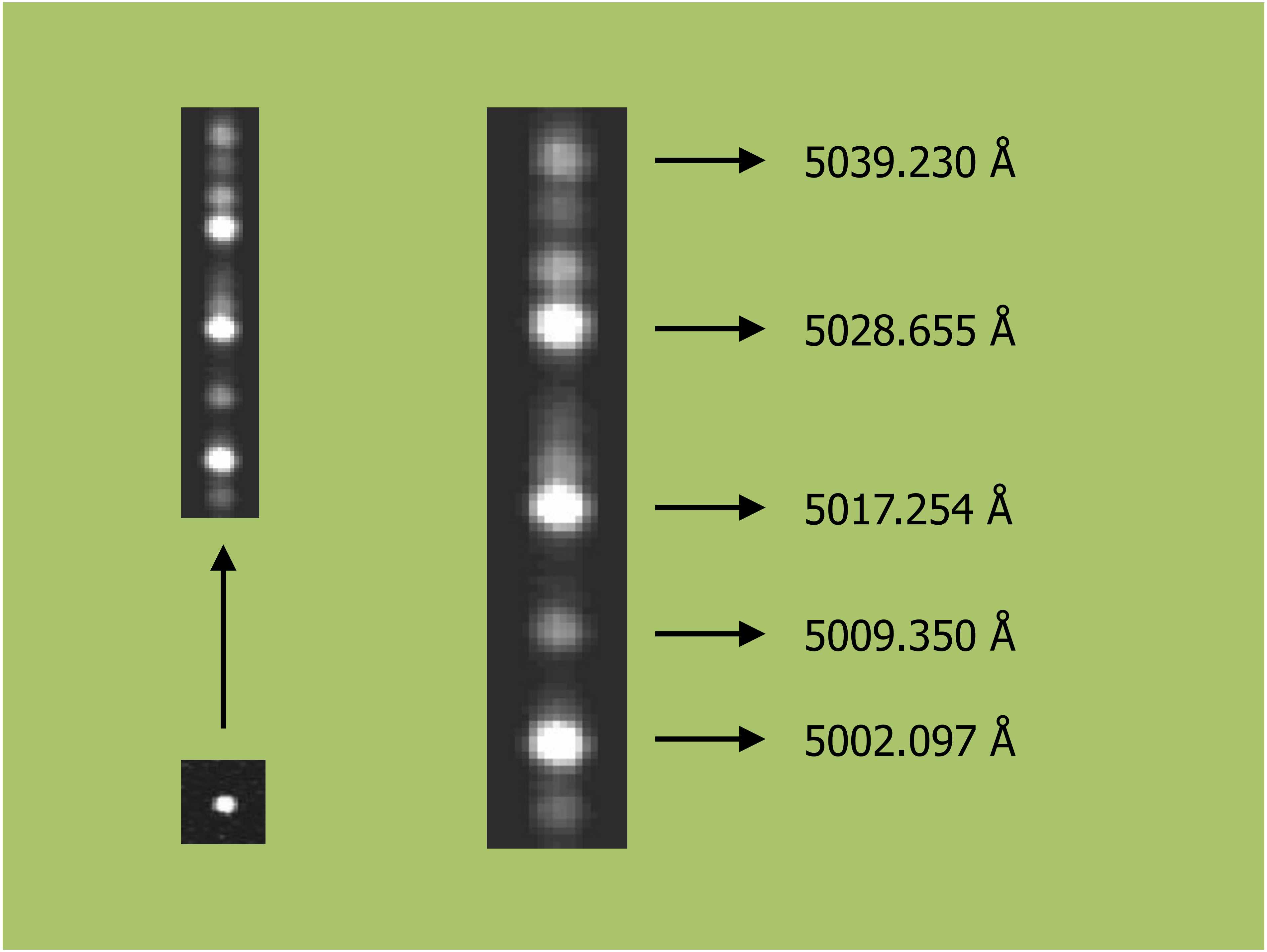

5039.230 Å
5028.655 Å
5017.254 Å
5009.350 Å
5002.097 Å

Radial velocity calculations

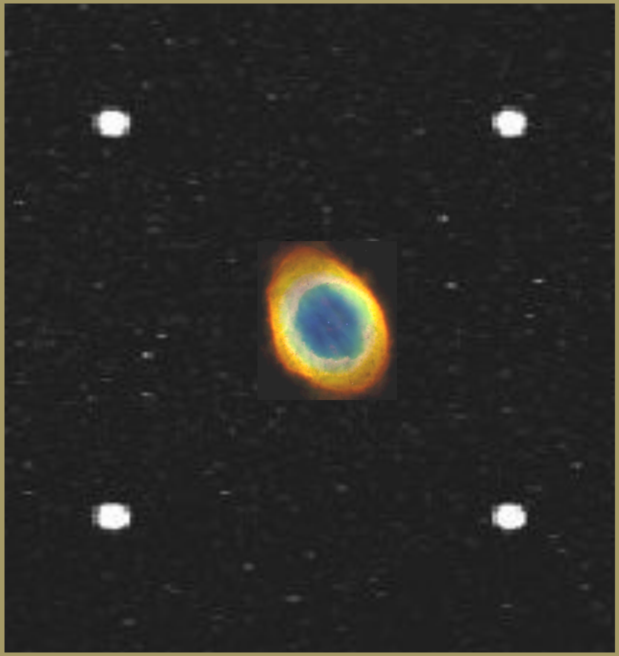

◇ Identify four closest calibration points that form a square around PN

◇ Calculate the redshifted wavelength of the [O III] emission feature at each of the four points

◇ Obtain the final wavelength by using a bilinear interpolation calculation – combining the four values according to the spatial relation of each of the 4 calibration points to the PN

◇ Final wavelength and heliocentric correction are used to calculate the radial velocity

Galaxies studied with FOCAS and/or FORS

Name	Type	PNs found	Distance
NGC 4697	E5	591	11 Mpc
NGC 1344	E5	197	19 Mpc
NGC 821	E5	167	19 Mpc
NGC 4649	E2	326	15 Mpc
NGC 5866	S0	242	15 Mpc
M 82	Edge-on S	109	4 Mpc
NGC 891	Edge-on S	125	10 Mpc
NGC 5907	Edge-on S	316	16 Mpc
NGC 4244	Edge-on S	not yet	5 Mpc
IC 10	dwarf Irr	35	0.7 Mpc

From fluxes to magnitudes

- We call I(5007) the nebular flux in erg cm^{-2} s^{-1}
- We can define "Jacoby magnitudes" in the following way:
  m(5007) = -2.5 log I(5007) -13.74
- The constant -13.74 is derived from the monochromatic flux of a star with V=0, and from the equivalent width of the Johnson V filter.
- Now we can build the PN luminosity function (PNLF): how many PNs are found at each apparent m(5007)

An example:
the PNLF of NGC 4697

The solid lines are Monte Carlo simulations of the PNLF for different total PN populations. I will explain how to build them in a minute.

Knowing the apparent mags(5007), we can build a histogram describing how many PNs there are within each bin of 0.2 mag.

Adopting a distance modulus and correcting for foreground extinction, we get the absolute mags, so that we can compare the observed PNLF (squares) with the simulations.

We find the best fit, giving total PN population and distance modulus.

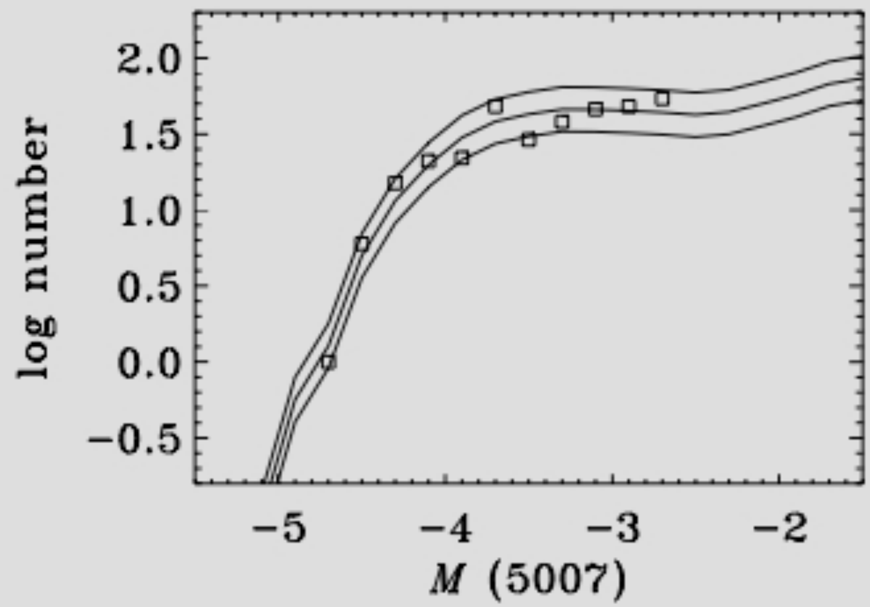

FIG. 14.—Observed [O III] λ5007 PNLF of NGC 4697 (*squares*), with the 328 data binned into 0.2 mag intervals. The apparent magnitudes $m(5007)$ have been transformed into absolute magnitudes $M(5007)$ by adopting an extinction correction of 0.105 mag and a distance modulus $m - M = 30.1$. The three lines are PNLF simulations (Méndez & Soffner 1997) for three different sample sizes: 2500, 3500, and 4900 PNs. From the sample size it is possible to estimate the PN formation rate (see text). The adoption of a distance modulus 29.9 or 30.3 instead of 30.1 would ruin the fit.

PNLF distance determination: the other way (Jacoby, Ciardullo)

- The other method is based on the assumption that the “bright end” of the PNLF has the same shape and absolute brightness everywhere.
- The universal bright end is represented by an exponential with cutoff at M(5007) = -4.54

Fitting the PNLF of M 81

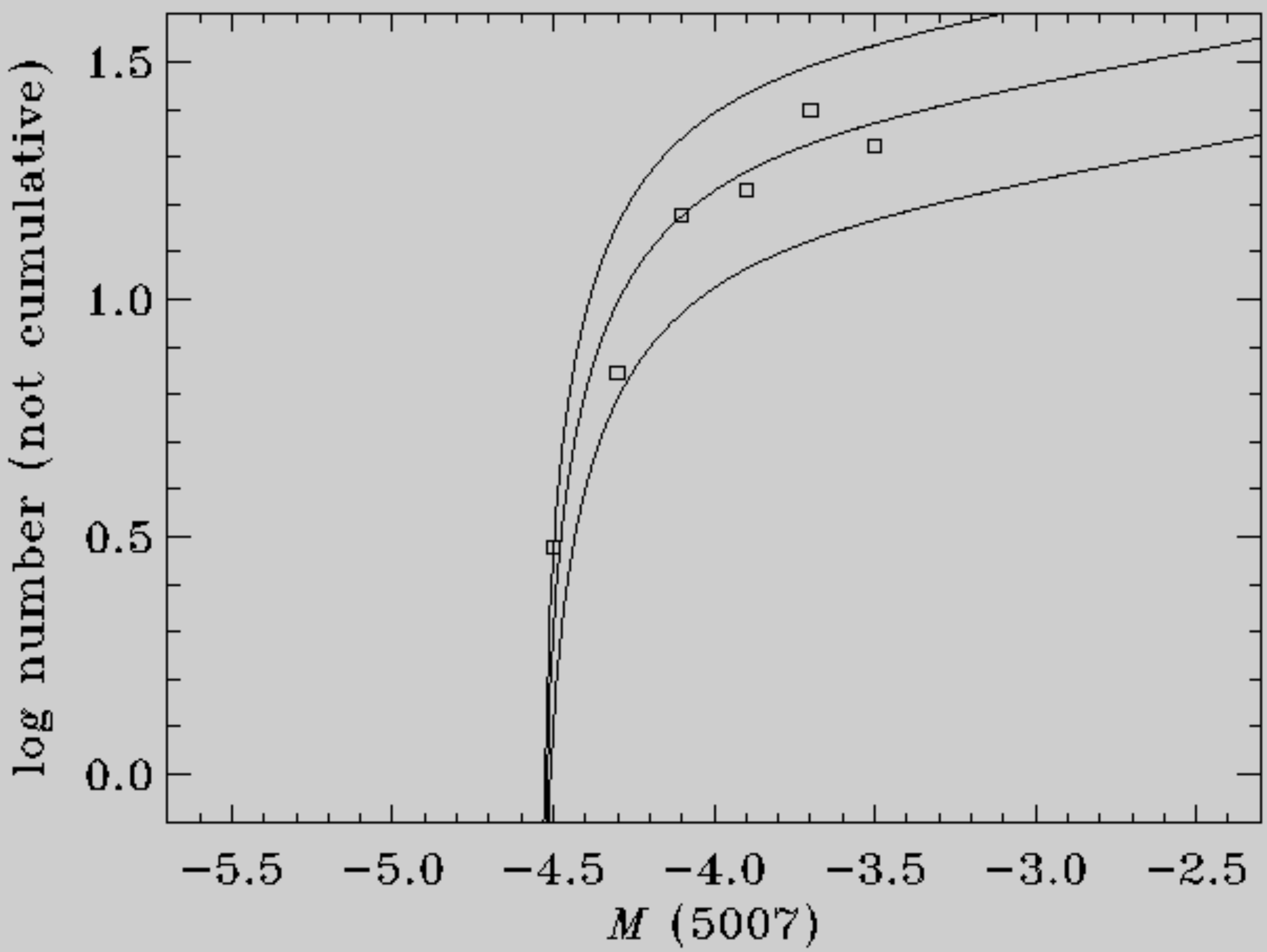

PNLF shapes

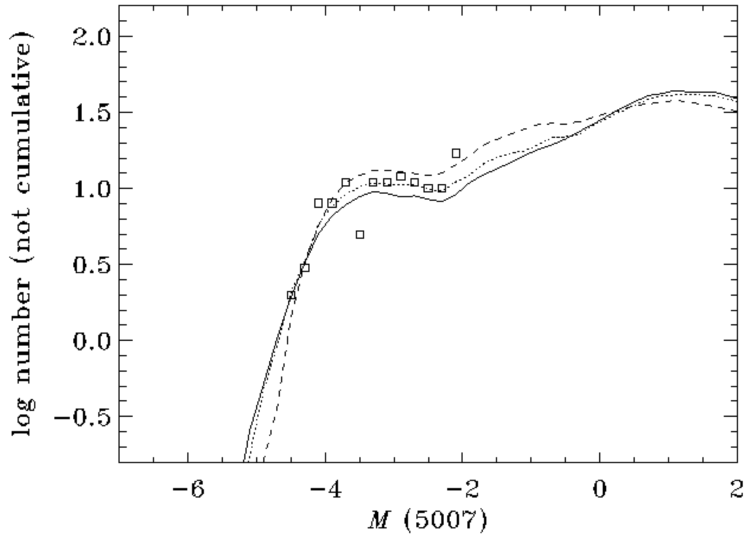

log number (not cumulative)
2.0
1.5
1.0
0.5
0.0
−0.5
−6
−4
−2
0
2
M (5007)

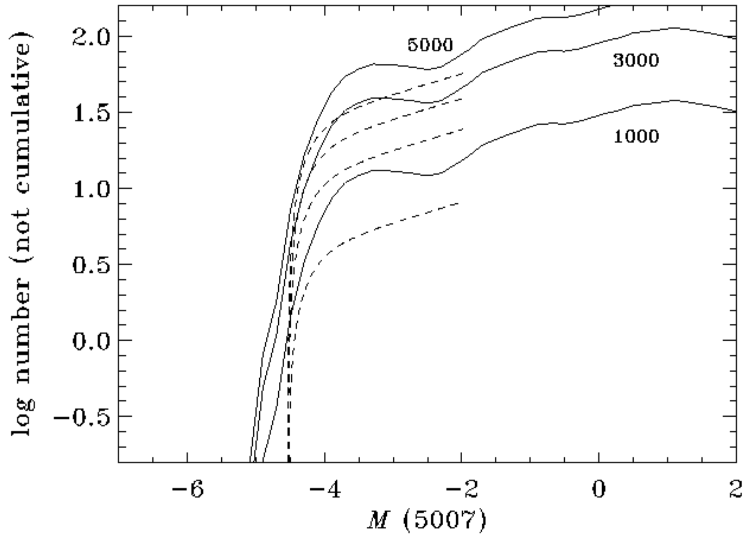

log number (not cumulative)
2.0
1.5
1.0
0.5
0.0
−0.5
5000
3000
1000
−6
−4
−2
0
2
M (5007)

Making PNLF simulations

This is a simulation of a collection of 1500 central stars burning H.

The evolutionary tracks show a quick drop in luminosity as the H-burning shell is extinguished and the star goes into the white dwarf cooling track. For that reason there is a lack of central stars at log L between 2.5 and 3.

This lack of central stars leads us to expect a lack of intermediate-brightness PNs.

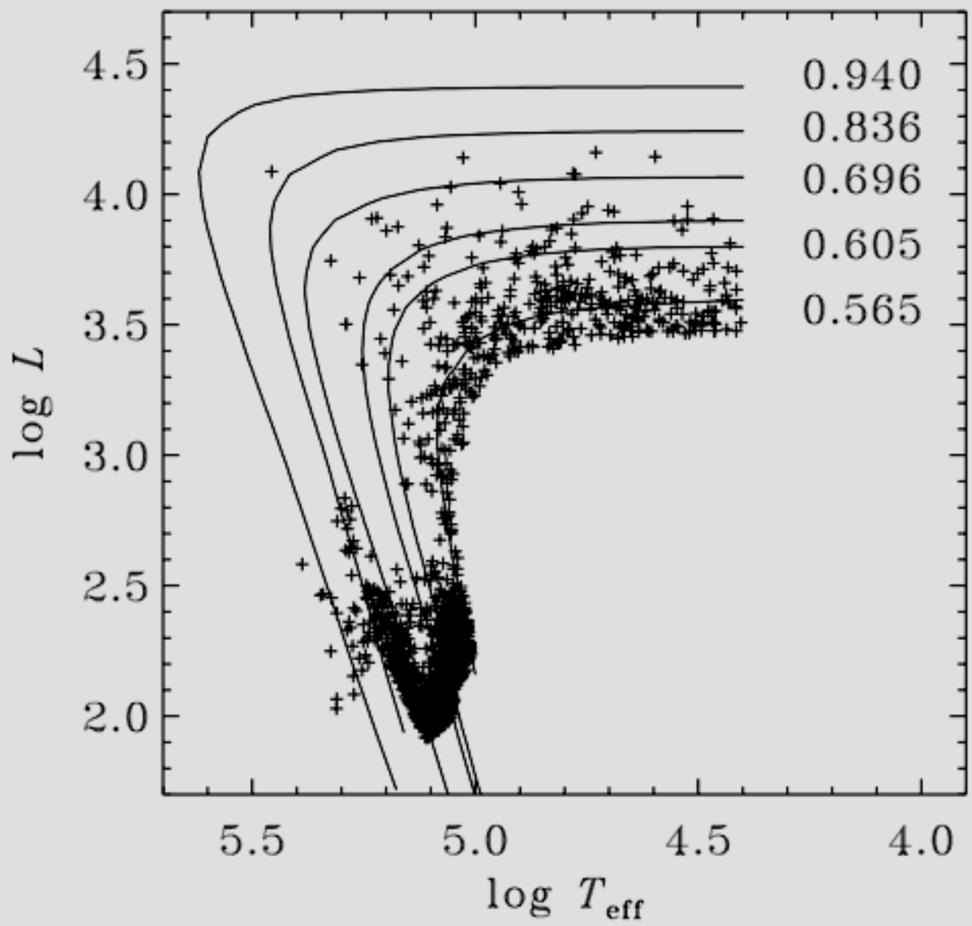

Monte Carlo simulations of PNLFs

- Generate a set of central stars with random post-AGB ages and masses.
- Using evolutionary tracks, derive the corresponding central star luminosities and surface temperatures.
- Using recombination theory and empirical information about leaking of H-ionizing photons, calculate the nebular Hbeta luminosities.
- Assuming a distribution of ratios 5007/Hbeta, obtain the luminosities in 5007 and compute the PNLF.

Monte Carlo simulations

R.H. Méndez & T. Soffner: Improved simulati

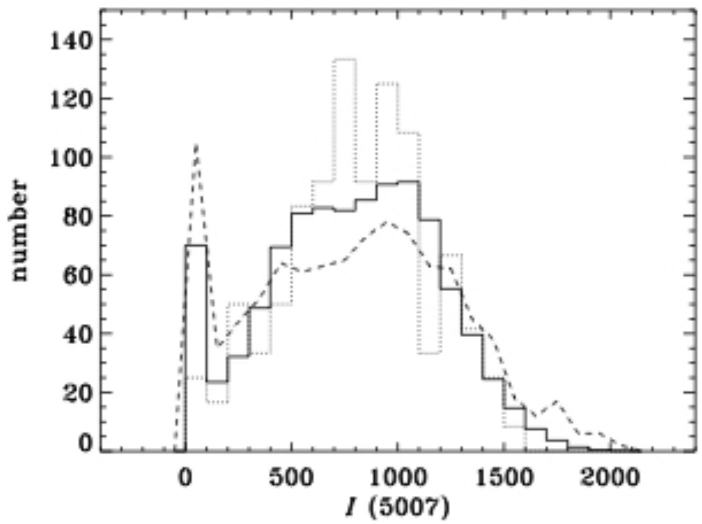

Fig. 3. Histograms of the intensity of $\lambda5007$ relative to $H\beta$, on the scale $I(H\beta) = 100$. The dashed line indicates the histogram for 983 objects in our Galaxy. The other two histograms have been normalized to this number. The dotted line is the histogram for 118 LMC objects. The full line is our simulated distribution, generated as described in the text.

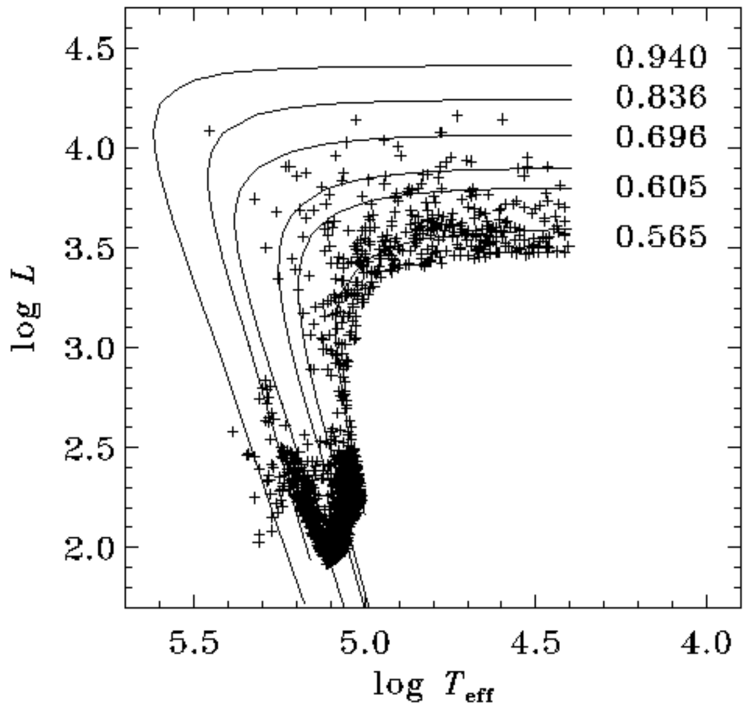

The age and mass distributions

- Post-AGB age: uniform random distribution from 0 to 30,000 years, counted from the moment when the stellar Teff becomes 25,000 K.
- Mass: from the IMF plus a constant SFR plus an initial-to-final mass relation we obtain exponential mass distributions with a maximum at 0.55-0.57 solar masses, decreasing towards larger masses. We assume that stars less massive than 0.55 solar masses evolve too slowly to produce visible PNs.
- For a population without recent star formation we cut the mass distribution at some maximum final mass, because all the initially more massive stars have already evolved into white dwarfs.

And now we empirically

…try to determine what maximum final mass we need to fit the observed PNLFs in different galaxies. The answer is about 0.63 solar masses for bulges of spirals like M 31 and also for elliptical galaxies (which is a very interesting problem).

It would be higher (about 1 solar mass) for galaxies with recent star formation. But the PNLF hardly changes (those massive central stars are quite rare).

Initial-final mass relation
Weidemann 2000, A&A 363, 647

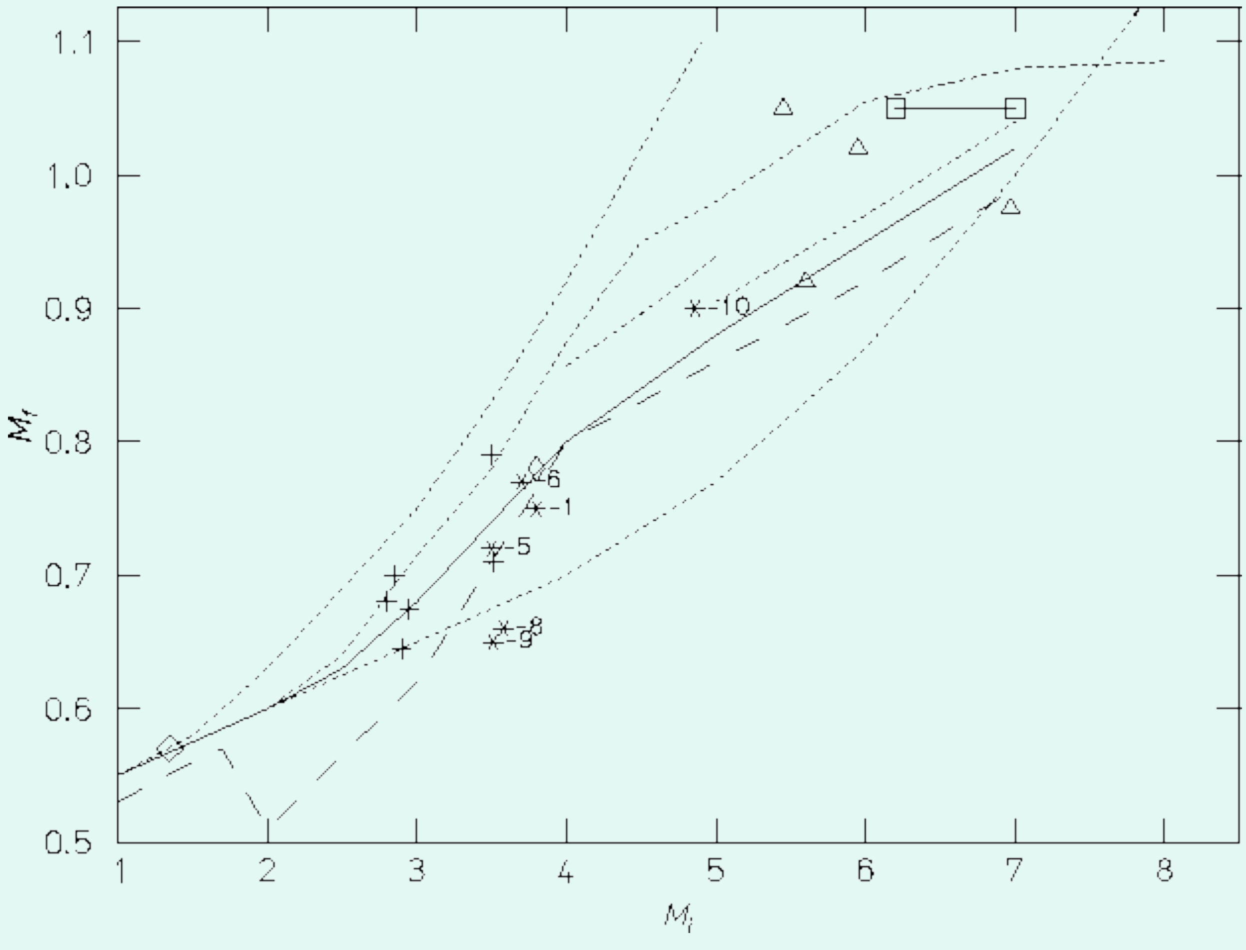

The unexplained fact

Since we expect ellipticals to have old populations, the initial mass is more or less 1 solar mass and the maximum final mass is expected to be 0.55 solar masses. Then the PNLF becomes very faint. In fact the galaxy would have trouble producing visible PNs; and indeed the specific PN formation rate is smaller in ellipticals than in spiral galaxies.

However, the PNLF bright end stays constant. The maximum final mass is observed to be ~0.63 Msun.

PNLF vs SBF distances

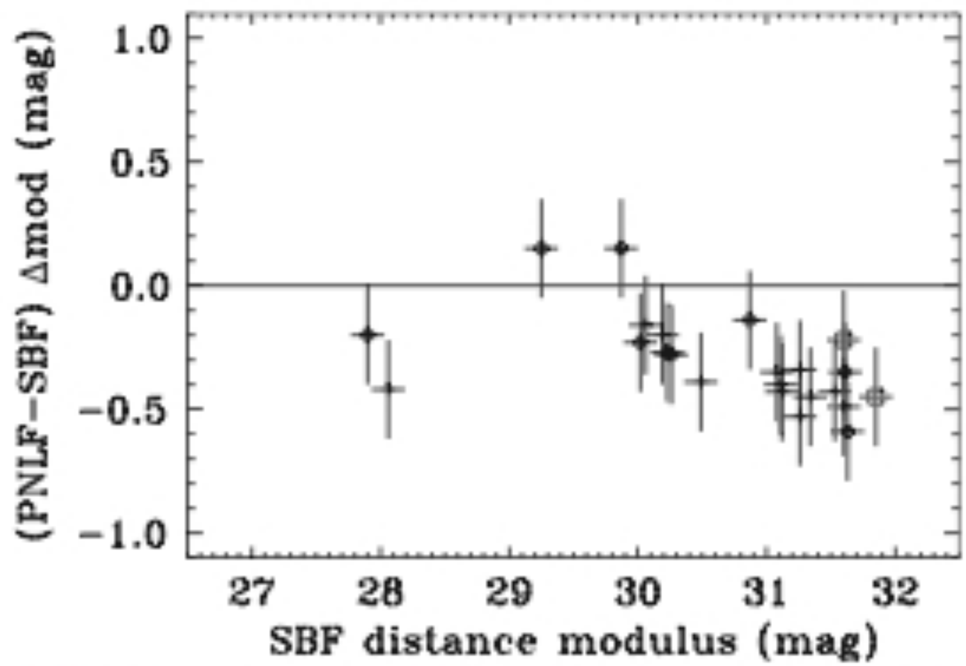

Figure 16. Difference between PNLF and SBF distance modulus plotted as a function of SBF distance modulus, for 23 galaxies. Non-elliptical galaxies are plotted as diamonds, while for ellipticals we show just the error bars. The two galaxies near $m - M = 28$ are NGC 5128 and M 81. The only two galaxies with a positive Δmod are NGC 4258 and NGC 3115. The agglomeration of galaxies between $m - M$ 31 and 32 is dominated by the Virgo and Fornax clusters. Our recent PNLF additions, ellipticals NGC 1344 in Fornax and NGC 821, are indicated as squares.

PNLF Distance of NGC 891

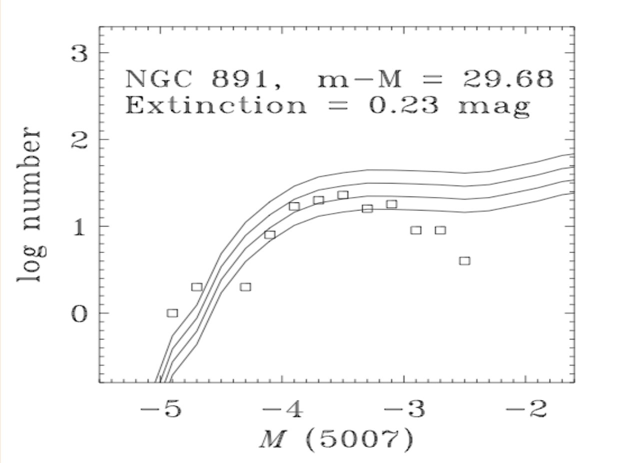

|Z| > 0 arcsec

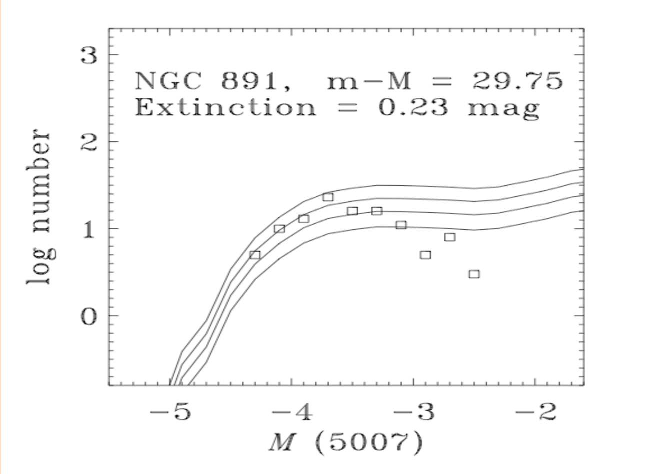

|Z| > 10 arcsec

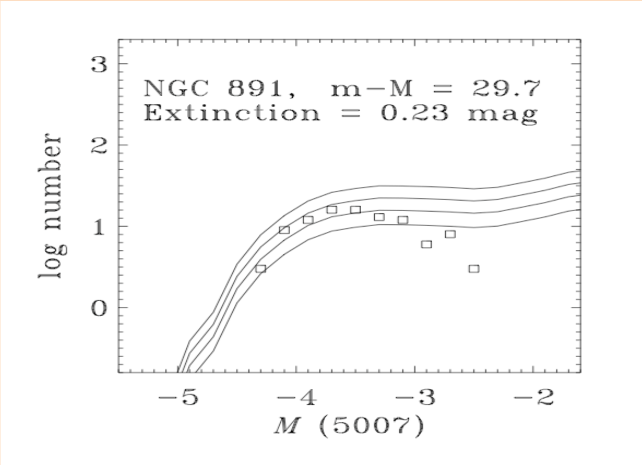

|Z| > 15 arcsec

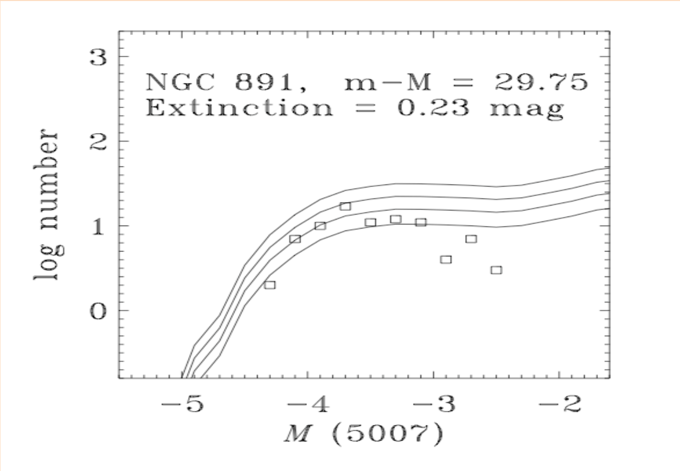

|Z| > 20 arcsec

Our best distance modulus: ***29.70 ± 0.20***

Ciardullo et al. (1991) with 33 PNs: ***29.97*** $^{+0.07}_{-0.11}$

Surface Brightness Fluctuation (SBF) distance (Tonry et al. 2001): ***29.61 ± 0.14***

Kinematic studies: the line-of-sight velocity dispersion in elliptical galaxies

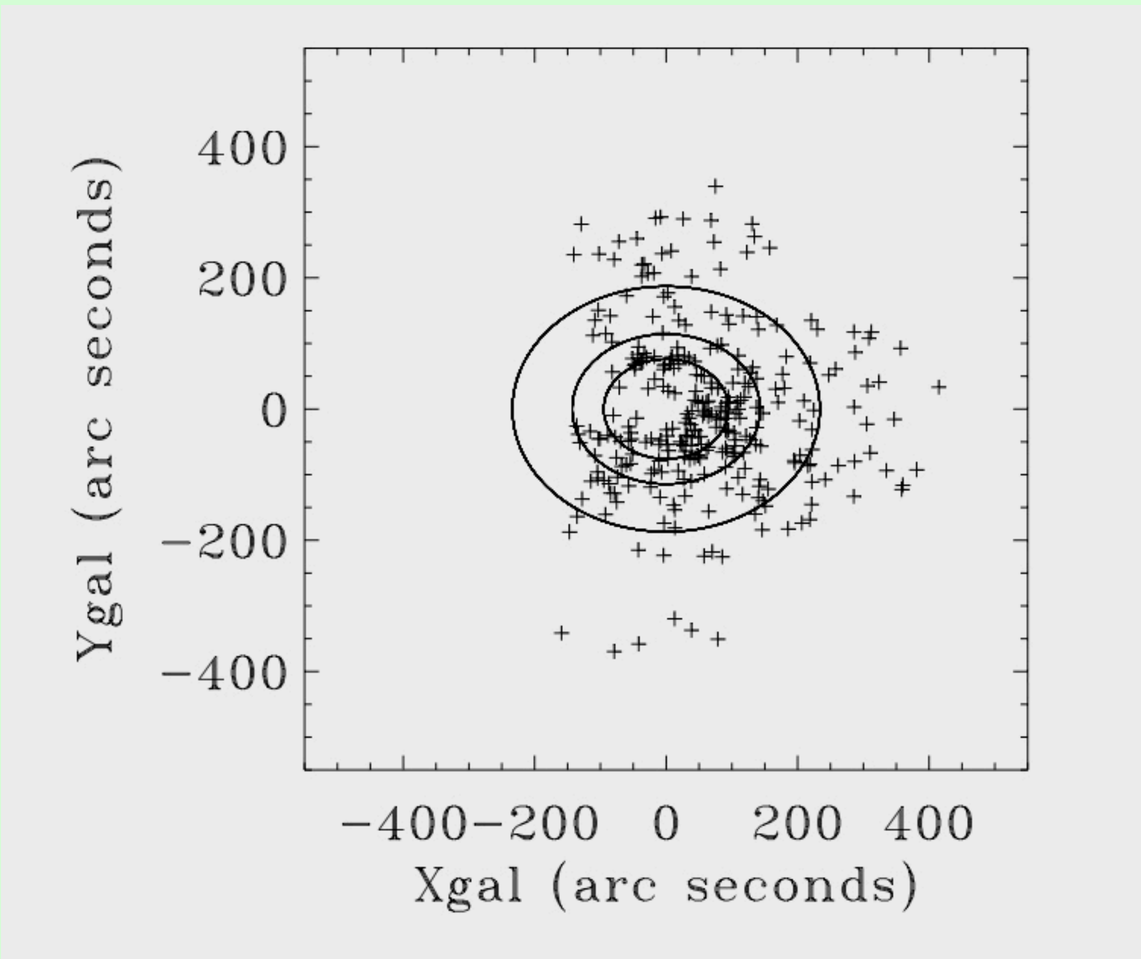

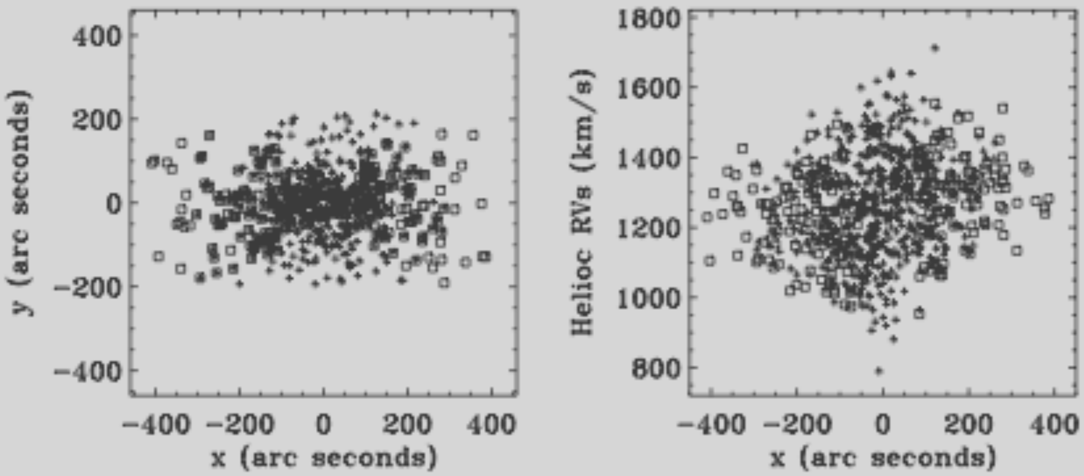

Figure 8. FORS (plus signs) and FOCAS (squares) PN detections. Left: positions of PNs relative to the center of light of NGC 4697, in arcsec. Right: radial velocities as a function of the *x* coordinates.

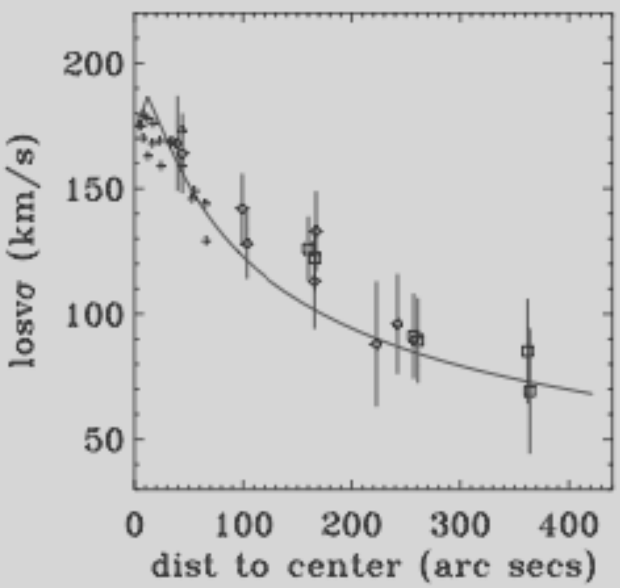

Figure 9. Line-of-sight velocity dispersion plotted as a function of average angular distance from the center of NGC 4697. Plus signs are measurements by Binney et al. (1990) on long-slit, integrated-light spectra along the major axis. Diamonds are PN results from Paper I. Squares are PN results from FOCAS radial velocities. The solid line is the Hernquist (1990) analytical model with a constant M/L ratio, adopting $R_e = 66$ arcsec, and a total mass of 1.5×10^{11} $M_{\odot}$. This is equivalent to $(M/L)_B = 9$.

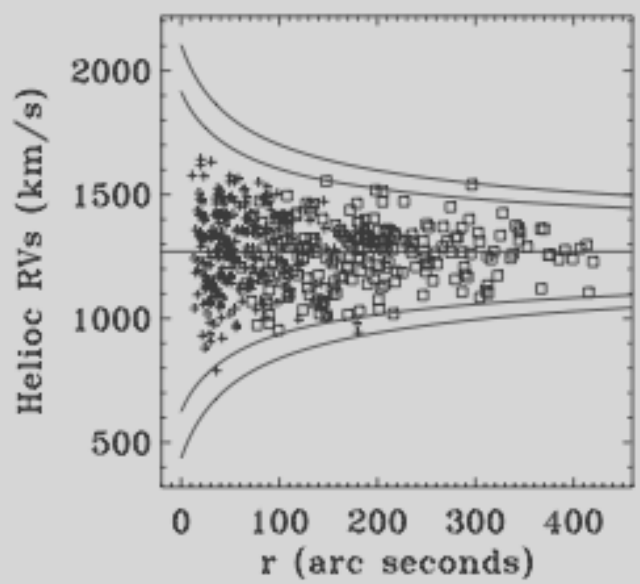

Figure 10. Individual FOCAS (squares) and FORS (plus signs) PN radial velocities plotted as a function of angular distance from the center of NGC 4697. We have only used FORS velocities of PNs from regions near the center, where we do not have FOCAS velocities. The solid lines are escape velocities for Hernquist models with $(M/L)_B = 9$ (outer) and 5 (inner).

Losvσ in NGC 4697, all PN data

- Plus signs: absorption-line data
- Diamonds: old FORS PN data.
- Squares: FOCAS PN data.

The solid line is a Hernquist model with a constant M/L ratio and a total mass of 1.5x10^11 Msun.

It still fits very well out to 5 Re (Re = 66 arc sec).
NGC 4697 remains the best case of quasi-Keplerian decline.

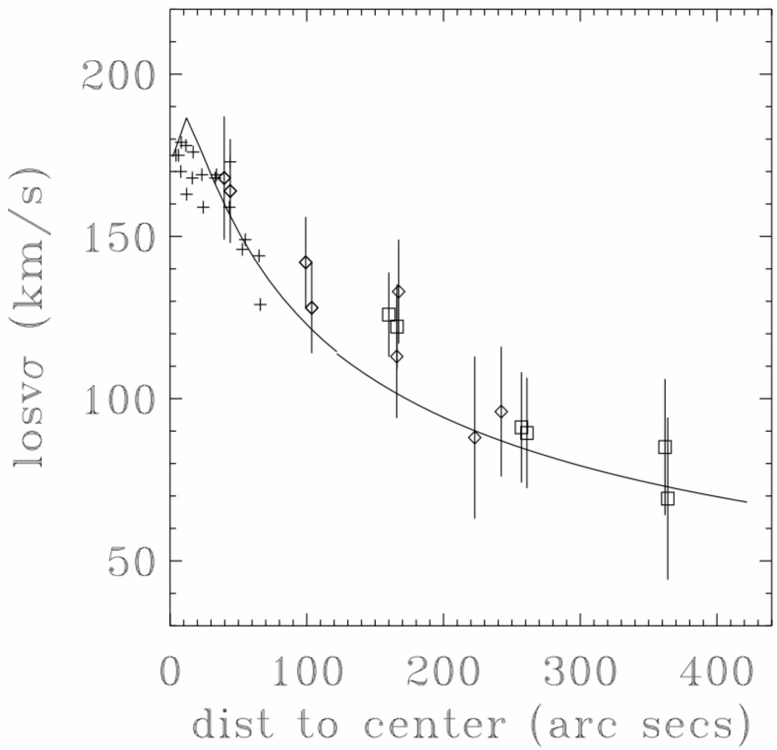

Escape velocities in NGC 4697

Individual FOCAS (squares) and FORS (plus signs) PN radial velocities plotted as a function of angular distance from the center of NGC 4697

The outer escape velocity line corresponds to (M/L)B = 9.

The inner one, to (M/L)B = 5.

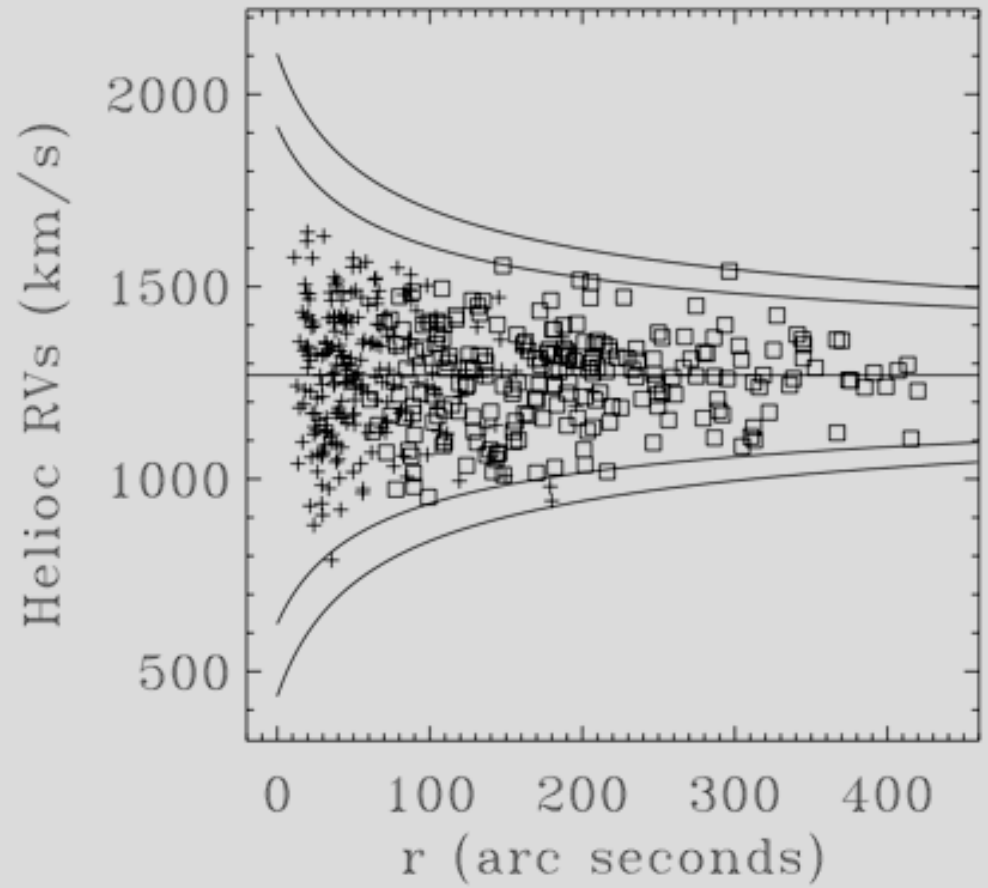

Quasi-Keplerian decline in NGC 821

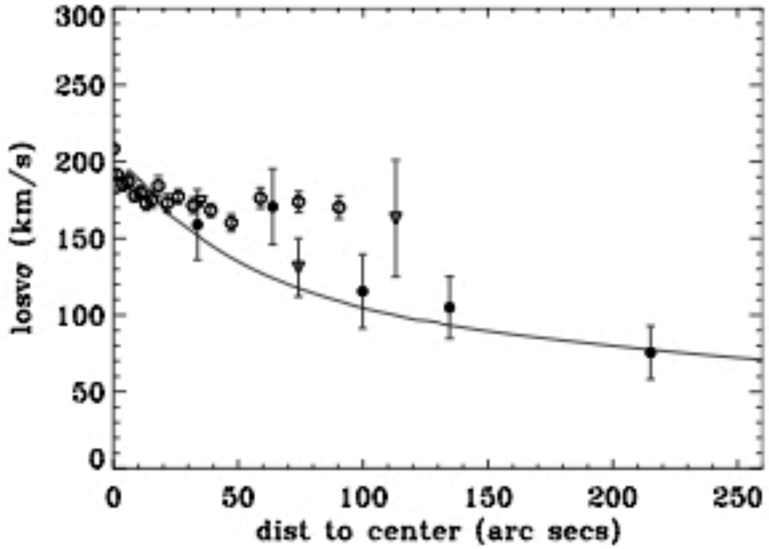

Figure 10. Line-of-sight velocity dispersion as a function of projected angular distance to the center of NGC 821 for the FOCAS + PN.S sample of 167 PNs (filled circles). The PNs were divided into 5 elliptical annuli as explained in the text. Overplotted are Sauron data (triangles; Weijmans et al. 2009) and Forestell & Gebhardt data (open circles). The solid line represents the analytical model of Hernquist (1990), with a constant M/L ratio, a total mass of $2 \times 10^{11}\ M_{\odot}$, and $R_e = 39''$.

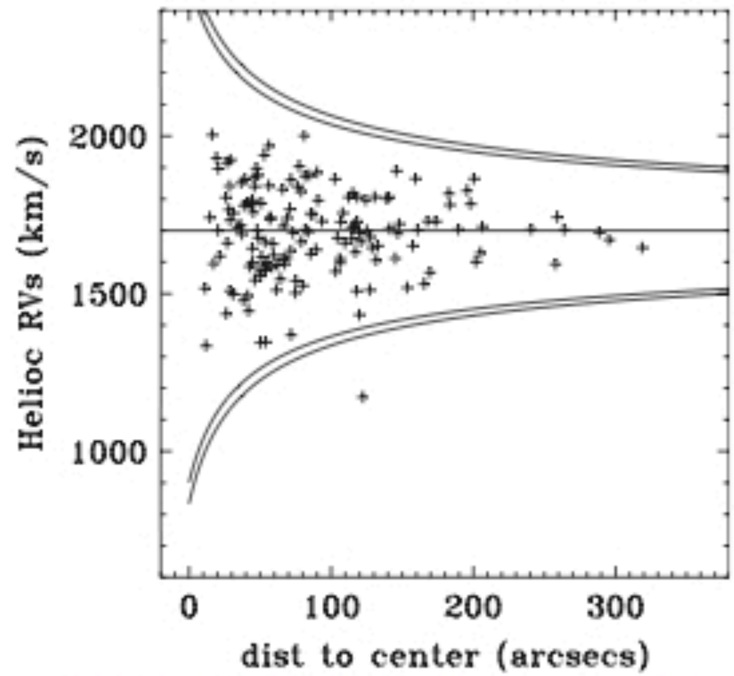

Figure 11. Individual PN radial velocities plotted as a function of angular distance from the center of NGC 821. The solid lines are escape velocities for Hernquist models with total masses $2.0 \times 10^{11}\ M_{\odot}$ (outer line) and $1.7 \times 10^{11}\ M_{\odot}$ (inner line). Note the outside position of the unrelated FOCAS object 104, which we have rejected as a PN. No other object has a velocity in excess

Escape velocities in NGC 5128 (Peng et al. 2004, ApJ 602, 685)

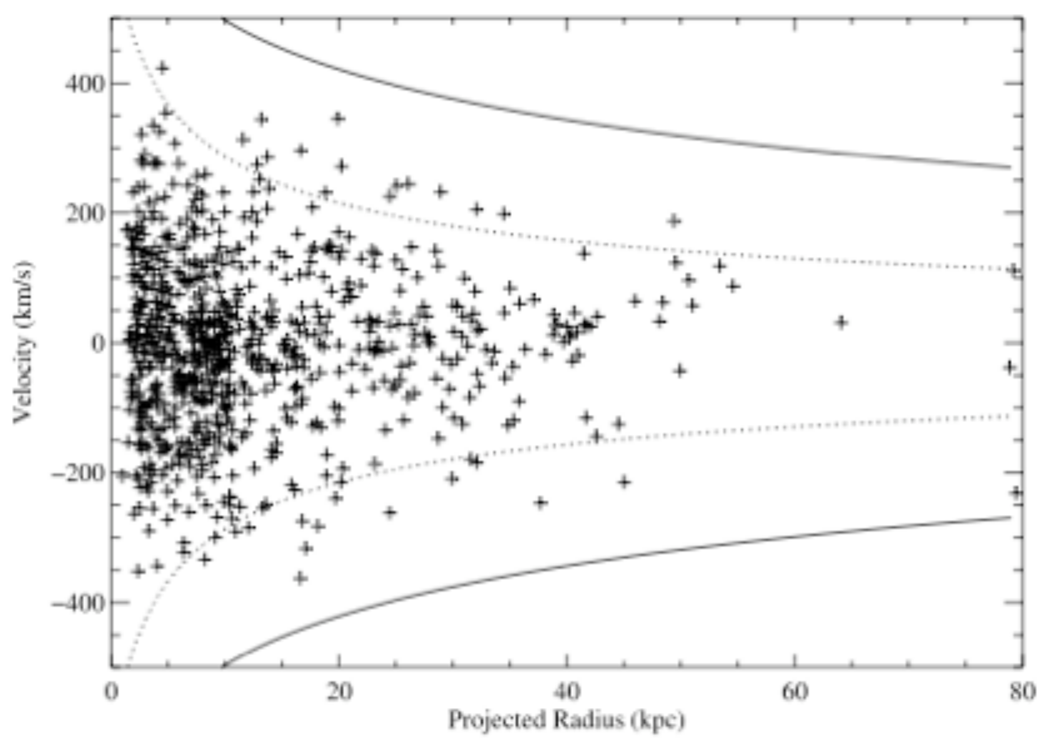

FIG. 12.—Escape velocity vs. radius for PNe. Each point marks the projected radius and radial velocity of a PN. The solid lines are the local escape velocity for our best-fit two-component Hernquist mass model. The dotted lines are the same, except for a model with no dark matter. Without dark matter, many PNe are unbound. With dark matter, even the most distant PNe are consistent with being bound.

Not all ellipticals misbehave

There are some intermediate-mass ellipticals that do show evidence of a dark matter halo:

NGC 5128 (Hui et al. 1995 ApJ 449, 592) confirmed by Peng, Ford and Freeman 2004, ApJ 602, 685. This one shows also significant halo rotation.

NGC 1344 (Teodorescu et al. 2005, ApJ 635, 290).

So now we have to answer another question: how frequent is the quasi-Keplerian behavior?

Hard to say, but perhaps 50% of the intermediate-mass ellipticals

Since we all want all galaxies to have dark matter halos, some people suggested that perhaps PNs were unreliable kinematic tracers (stars that do not behave as stars)

But PNs are good kinematic tracers

- M 82: Johnson et al., ApJ 697,1138
- NGC 891: Shih & Méndez, ApJ 725,L97
- IC 10: Gonçalves et al., MNRAS 425,2557
- NGC 5907, in preparation

- In all these cases, PN kinematics agree globally with other existing tracers, like HI, CO or Hα, where available. Sometimes a few PNs do something funny, for example in NGC 891.

NGC 891

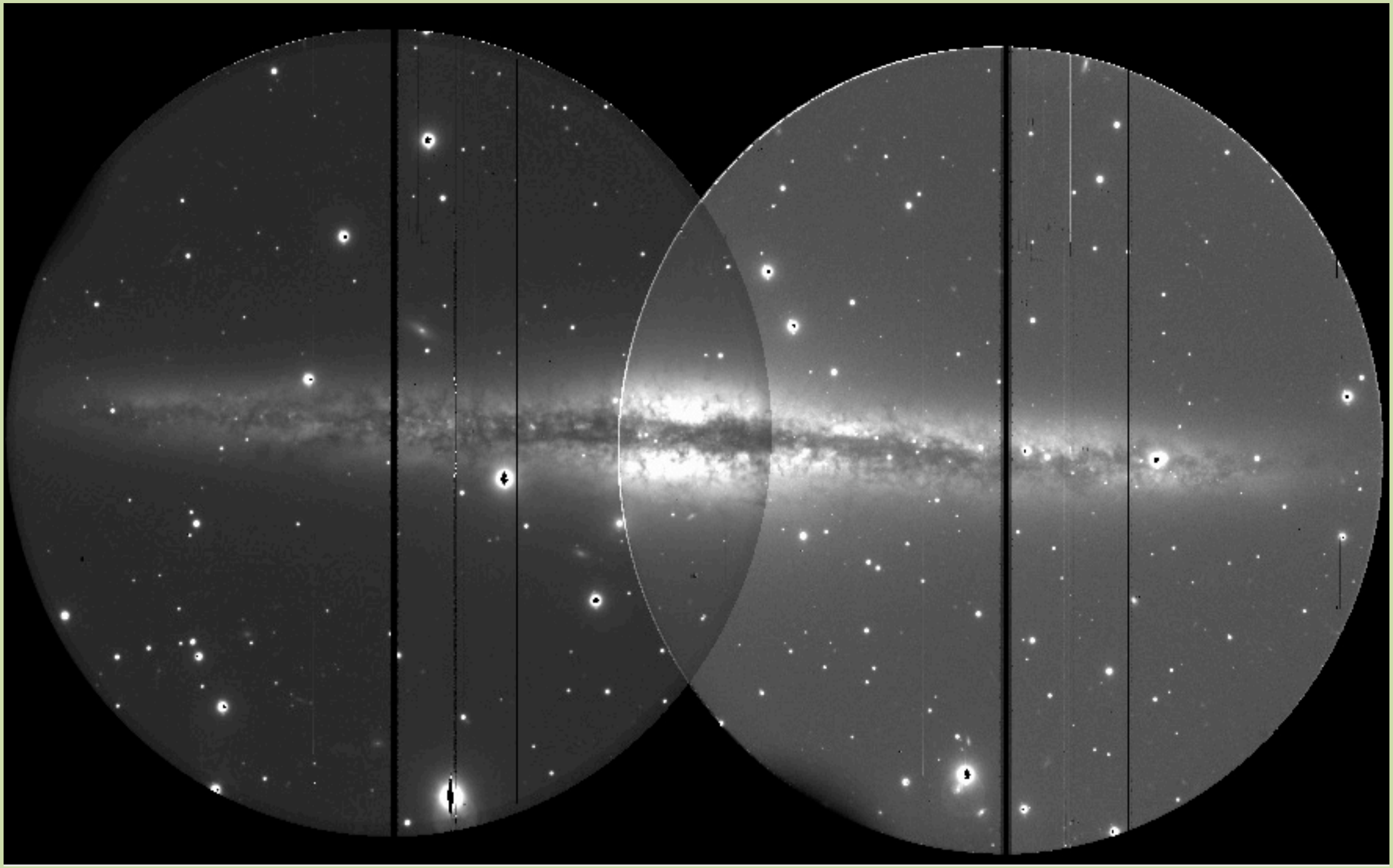

Data taken using Subaru FOCAS

Position-Velocity Map

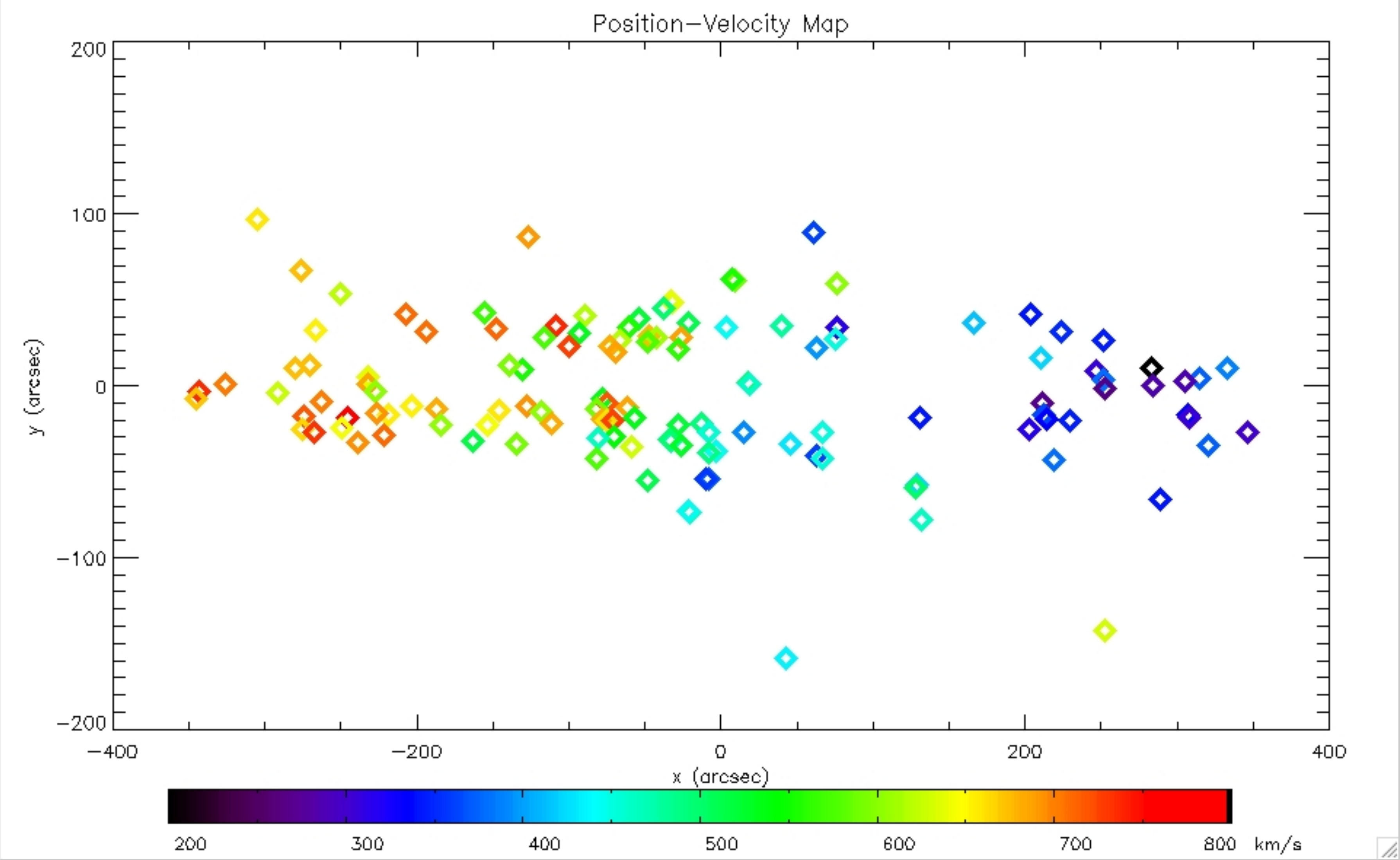

125 PNs in NGC 891

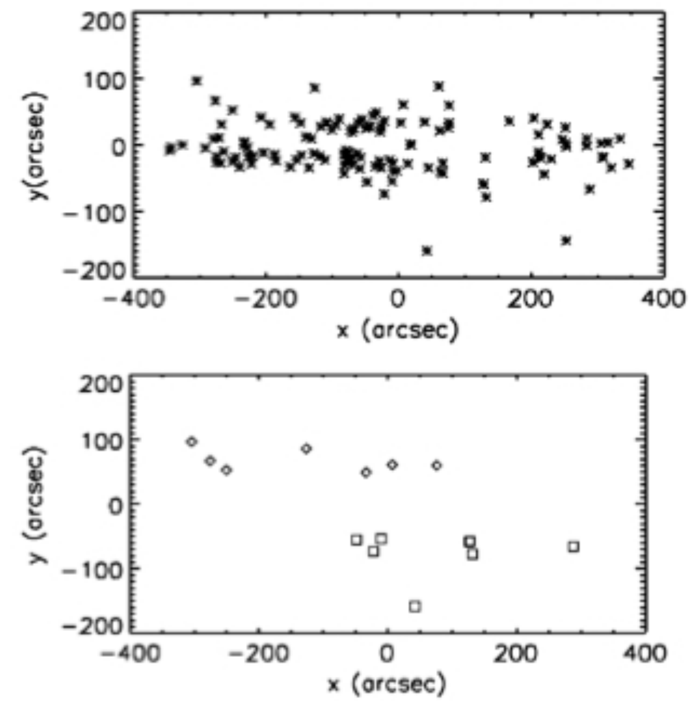

Figure 2. Upper panel: positions of all the PNs on the plane of the sky. The *x*-axis runs along the major axis of NGC 891 in the direction of increasing R.A.; the *y*-axis runs along the minor axis in the direction of increasing declination. Lower panel: positions of the two "excess" groups on the plane of the sky. The squares with negative *y* coordinates are approaching PNs, and the diamonds with positive *y* coordinates are receding PNs (see the text).

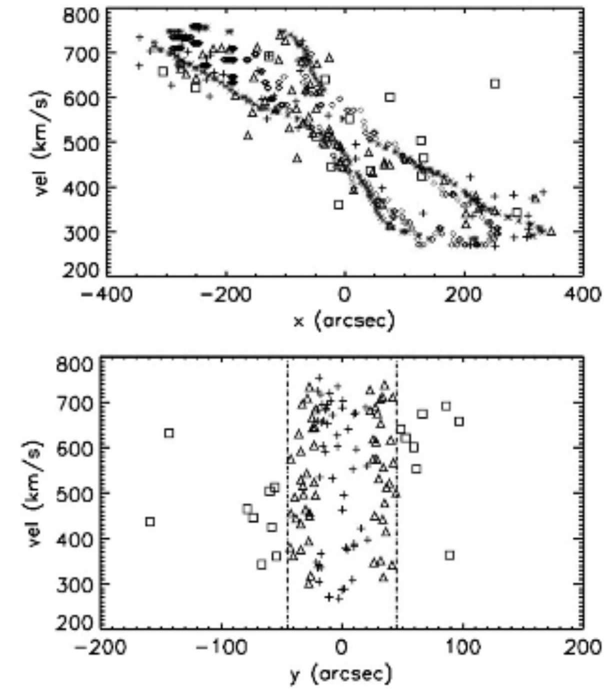

Figure 3. PN velocities plotted against *x* coordinates (above) and against *y* coordinates (below). The velocity gradient along the *x*-axis indicates a rotating disk, as expected. PNs represented as plus signs are within 1 kpc of the galactic plane. Triangles indicate PNs located between 1 and 2 kpc from the plane. Squares are PNs more distant than 2 kpc from the plane. Asterisks outline the HI data from Figure 6 in Oosterloo et al. (2007). Diamonds outline the Hα data from Figure 8 in Kamphuis et al. (2007b). The black shapes at the upper left are accumulations of diamonds. The position-velocity diagram of the PNs roughly agrees with the HI and Hα observations. In the lower panel, we see the "excess" of approaching PNs at large negative *y* and receding PNs at large positive *y*.

Stellar Streams in Spirals

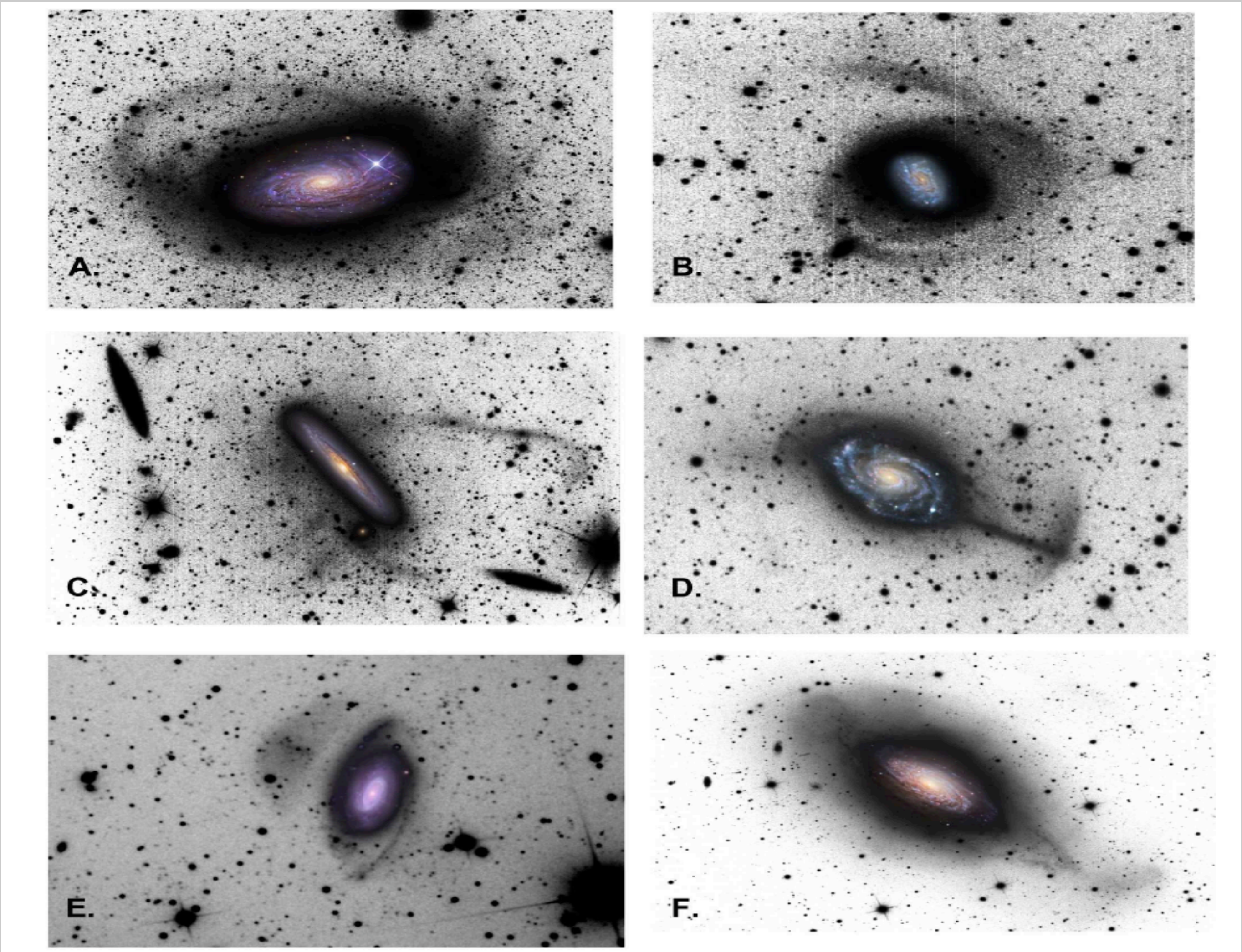

Martinez-Delgado et al. 2010

Ring Structure around NGC 5907

Past Minor Mergers

- These two groups may be remnants of minor mergers
- Evidence of past minor mergers in NGC 891:
  - Clumps of over-density in number of stars far from galactic plane
  - Large arcs and thick 'cocoon' surrounding the disk (Mouhcine et al. 2010)

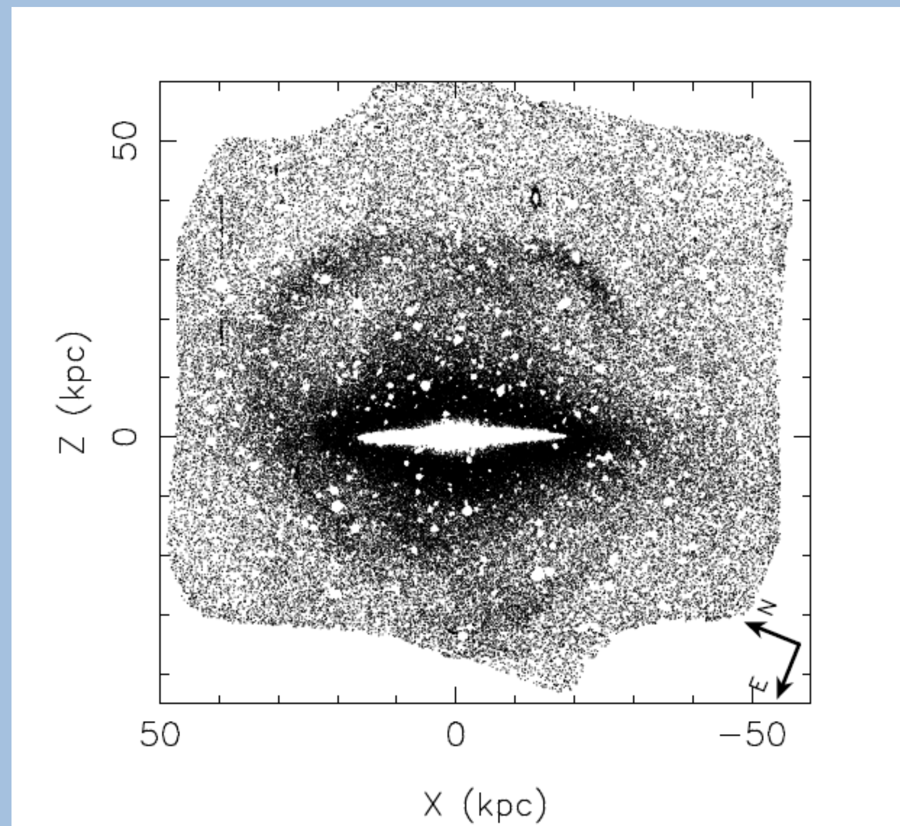

Mouhcine et al. 2010

The starburst galaxy M 82

Positions of PNs relative to the center of M 82. The x-axis runs along the major axis.

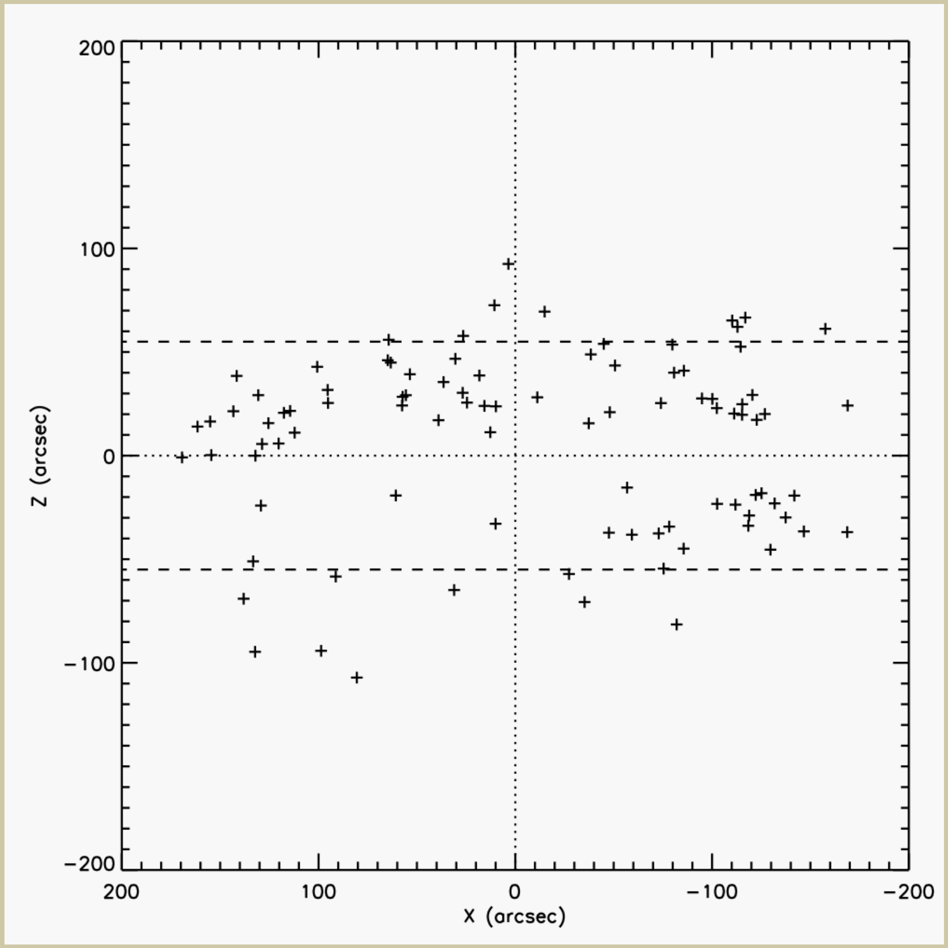

M 82: PN radial velocity vs x coord for z<30” (left) and z>55” (right)

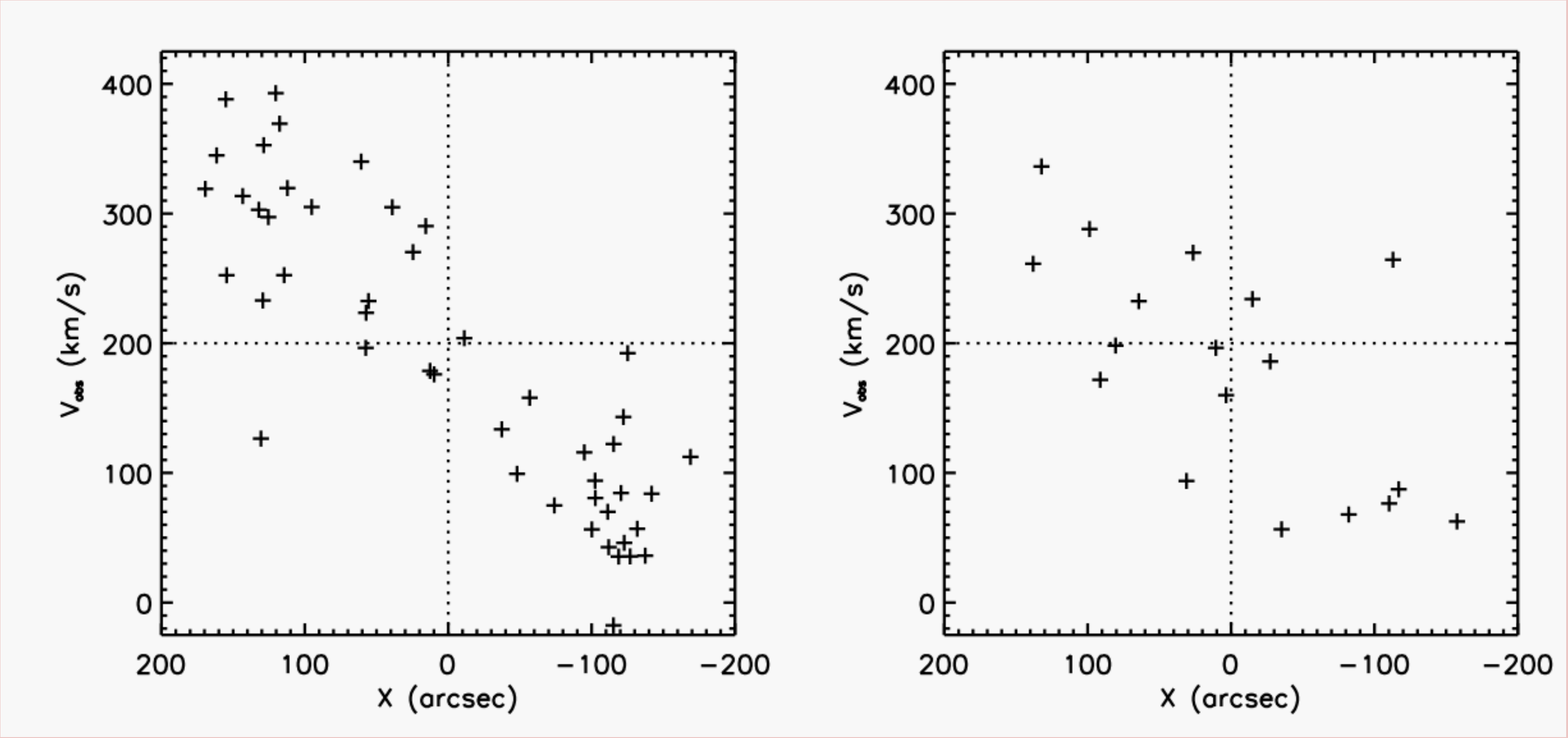

Dark matter in M 60

In some elliptical galaxies we know, from other evidence, that a dark matter halo is present. Will PNs confirm this presence? This is what we wanted to test in M 60 (Teodorescu et al. 2011 ApJ 736, 65; Das et al. 2011 MNRAS 415, 1244).

The evidence of dark matter in M 60 comes from XMM-Newton and Chandra X-ray data, plus globular cluster kinematics.

This was a combined effort, VLT + FORS, and Subaru + FOCAS.

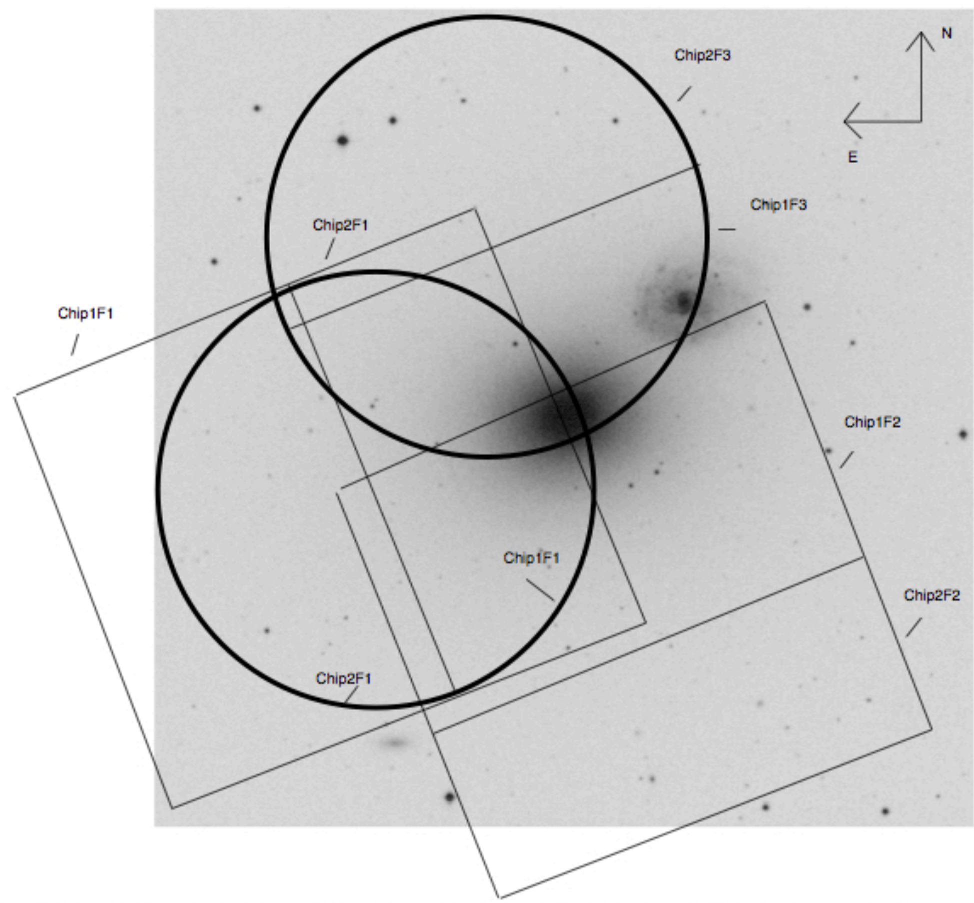

Figure 1. Fields F1, F2, and F3 observed for this project. The circular fields correspond to FOCAS, and the rectangular ones to FORS2. The spiral galaxy is NGC 4647. The total area of the sky shown here is 12.9 × 12.9 arcmin.

NGC 4649 (M 60)

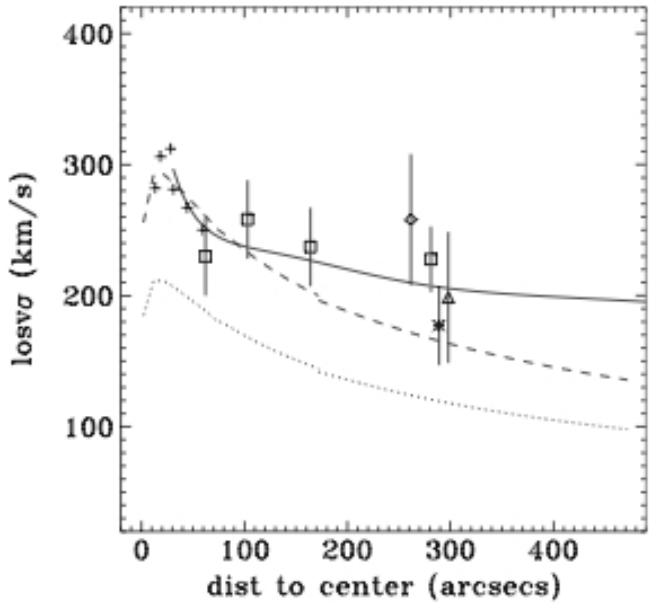

Figure 12. LOSVσ plotted as a function of average angular distance to the center of M 60. The PNs were divided into four regions, as explained in the text. These four data points are represented as squares. In addition, there is a diamond for PNs with large positive y, a triangle for PNs with large negative y, and an asterisk for PNs with large positive x. Plus signs are major-axis, long-slit absorption-line data (Fisher et al. 1995; Pinkney et al. 2003). The dotted line represents the analytical model of Hernquist (1990), with a constant M/L ratio, a total mass of $6 \times 10^{11}\ M_{\odot}$, and $R_e = 128''$. The dashed line is the same kind of model, but with a higher mass of $1.15 \times 10^{12}\ M_{\odot}$. The solid line is a two-component Hernquist mass distribution, as described in the text.

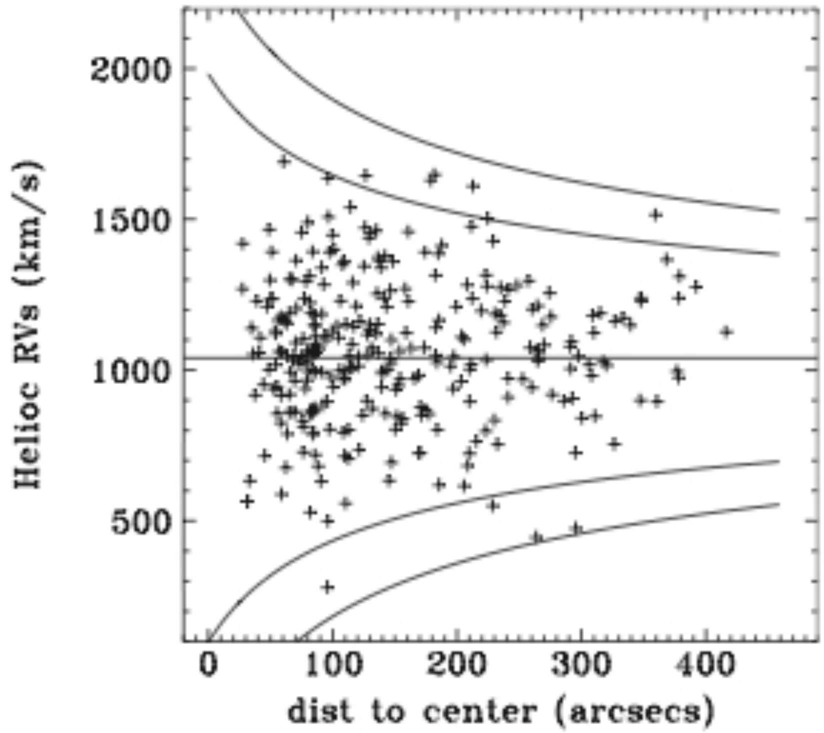

Figure 13. Individual PN radial velocities plotted as a function of angular distance from the center of M 60. The solid lines are escape velocities for Hernquist models with total masses $1.2 \times 10^{12}\ M_{\odot}$ (outer lines) and $6 \times 10^{11}\ M_{\odot}$ (inner lines).

Losvσ in NGC 4697, all PN data

- Plus signs: absorption-line data
- Diamonds: old FORS PN data.
- Squares: FOCAS PN data.

The solid line is a Hernquist model with a constant M/L ratio and a total mass of 1.5x10^11 Msun.

It still fits very well out to 5 Re (Re = 66 arc sec).
NGC 4697 remains the best case of Keplerian decline.

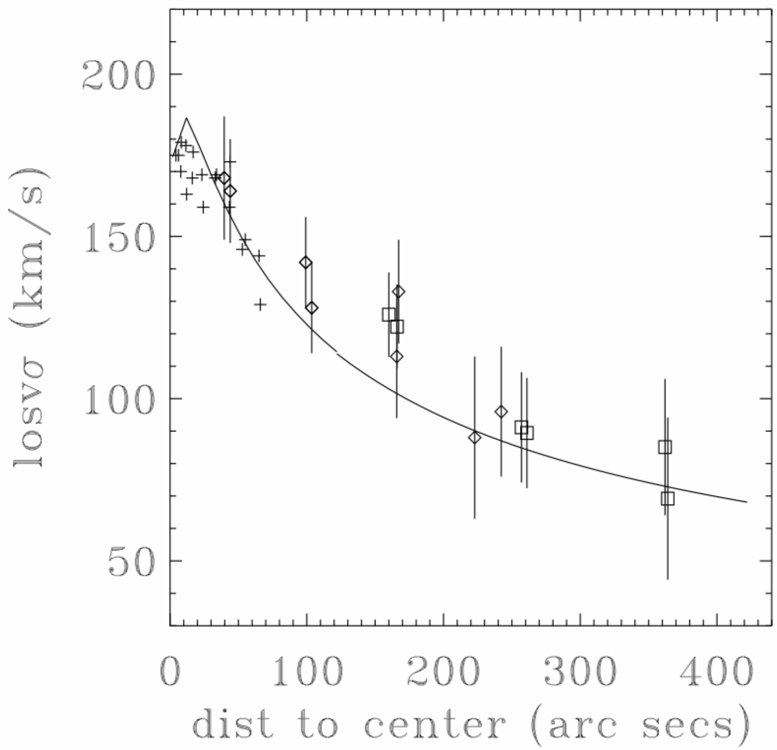

Dynamical analysis with NMAGIC

- De Lorenzi et al. (2008 MNRAS 385, 1729) showed that, if we <u>assume</u> modest radial anisotropy, we can fit the losvσ data in NGC 4697 with models including dark matter halos.
- Unfortunately, isotropic models <u>without</u> dark matter also fit.
- The same situation in NGC 821. It has not been possible to break this no dark matter – anisotropy degeneracy.

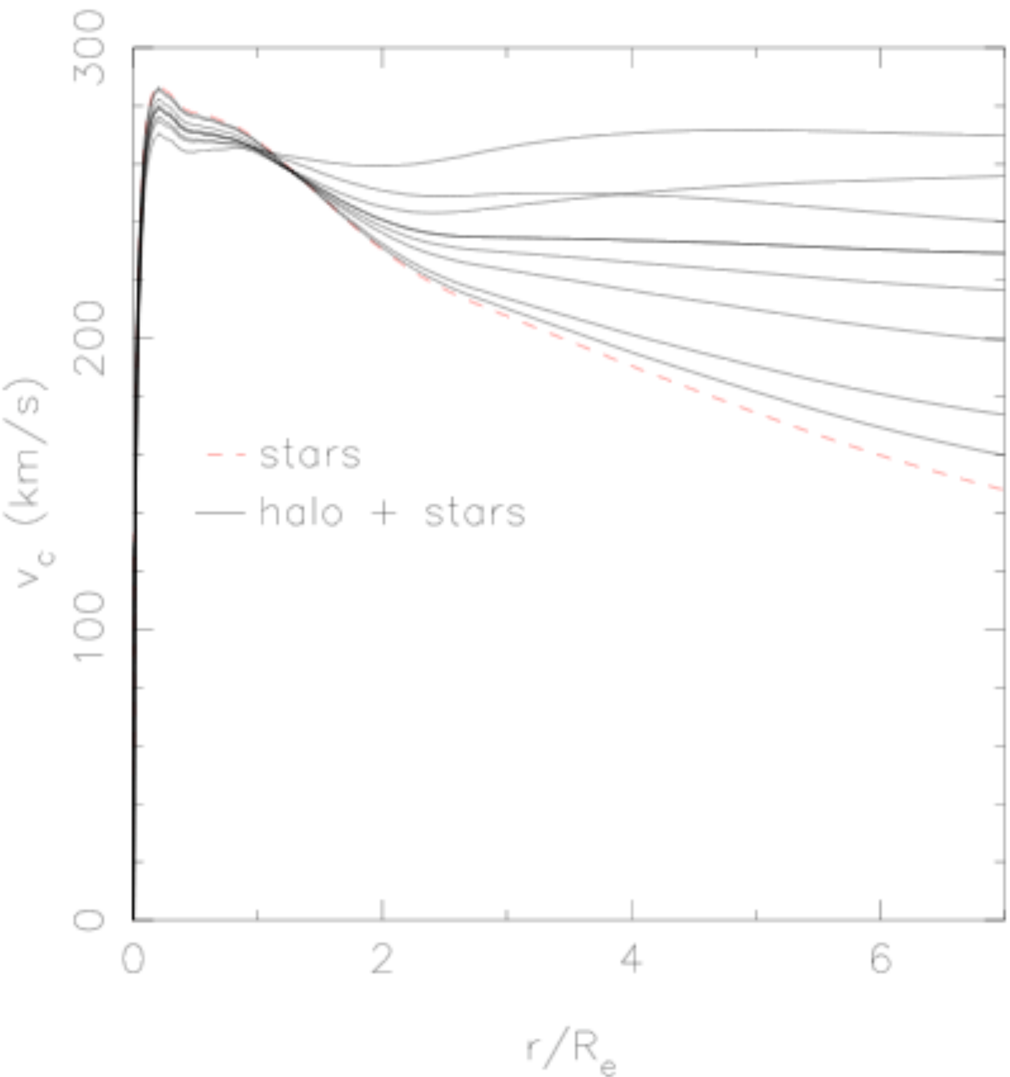

Figure 15. Circular velocity curves of the potentials used in the modelling, including the self-consistent model A (dashed line), and a sequence of dark matter halos (solid lines). The lines at $r/R_e = 7$ run from model A (bottom) to K (top), with models F and G represented by the same curve; *cf.* Table 1.

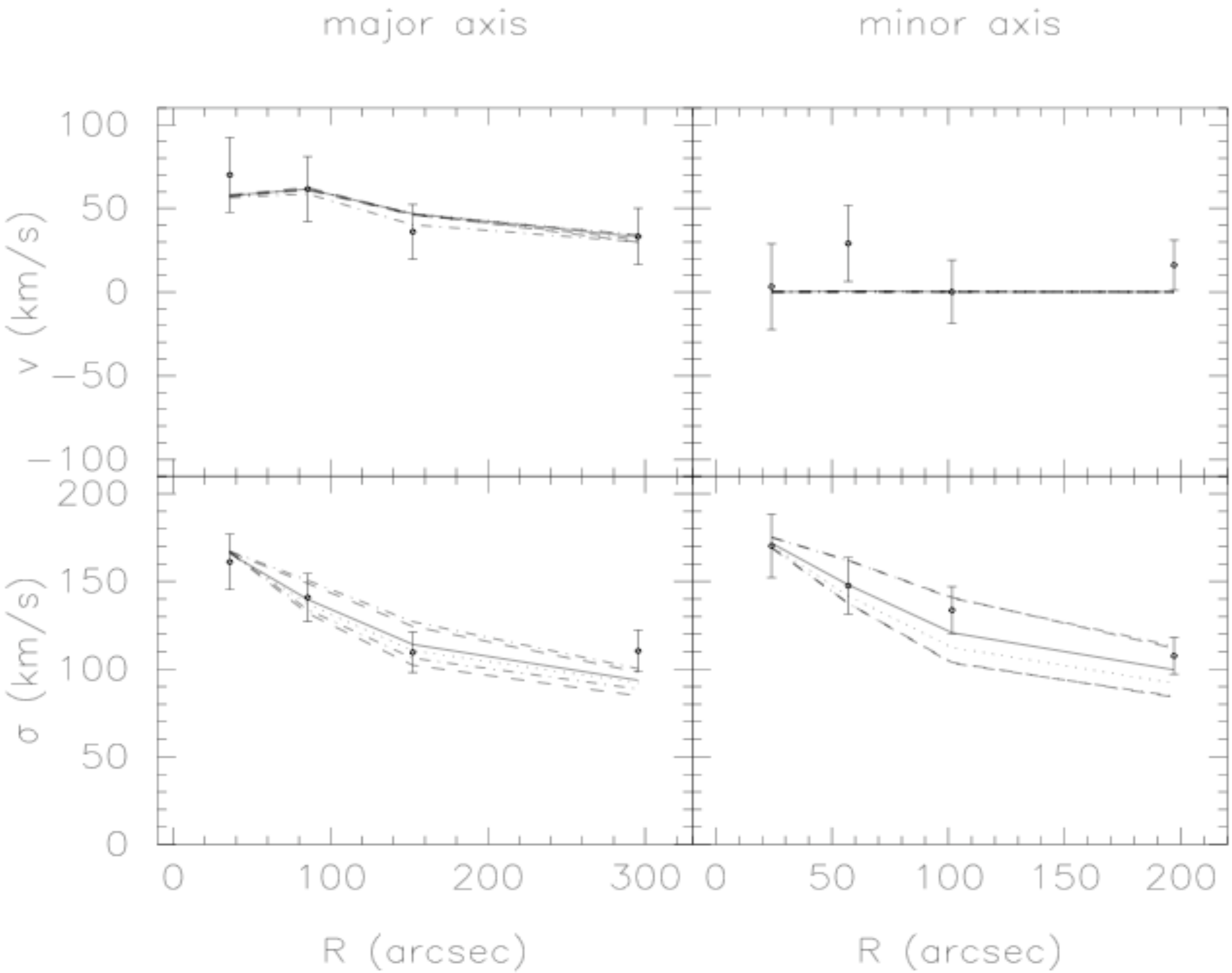

Figure 18. Comparison of the PNe velocity and velocity dispersion data (PND1, points) with models A, D, G, and K. Top left: v along the positive major axis. Top right: The same for the minor axis. Bottom left: σ along the positive major axis. Bottom right: The same but for the minor axis. Dashed, dotted, full, and upper dashed lines show models A, D, G, and K; the two dash-dotted lines show the variants of models A and K obtained with the likelihood scheme for the PNe.

Losvσ in NGC 4697, all PN data

- Plus signs: absorption-line data
- Diamonds: old FORS PN data.
- Squares: FOCAS PN data.

The solid line is a Hernquist model with a constant M/L ratio and a total mass of 1.5x10^11 Msun.

It still fits very well out to 5 Re (Re = 66 arc sec).
NGC 4697 remains the best case of Keplerian decline.

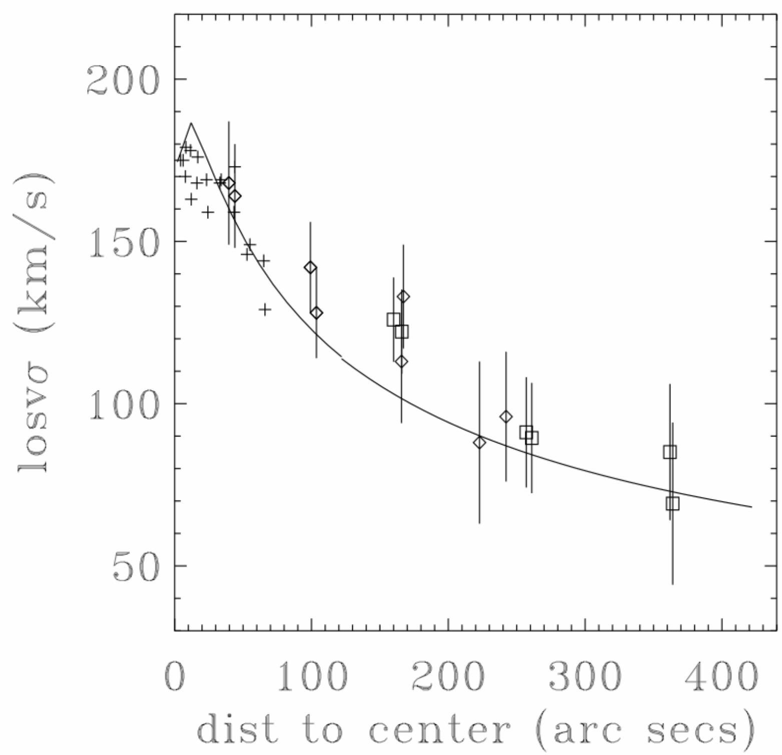

A final test of radial anisotropy?

Build numerical simulations of a stellar population moving in the potential of a mass distribution that includes a dark matter halo.

Impose a degree of radial anisotropy that will mask the dark matter and produce a Keplerian decline of losvσ.

Build a velocity histogram.

In the outskirts of the stellar distribution, the histogram will be "peaky" because most of the motion happens perpendicular to the line of sight.

Near the center, the histogram will be flatter…

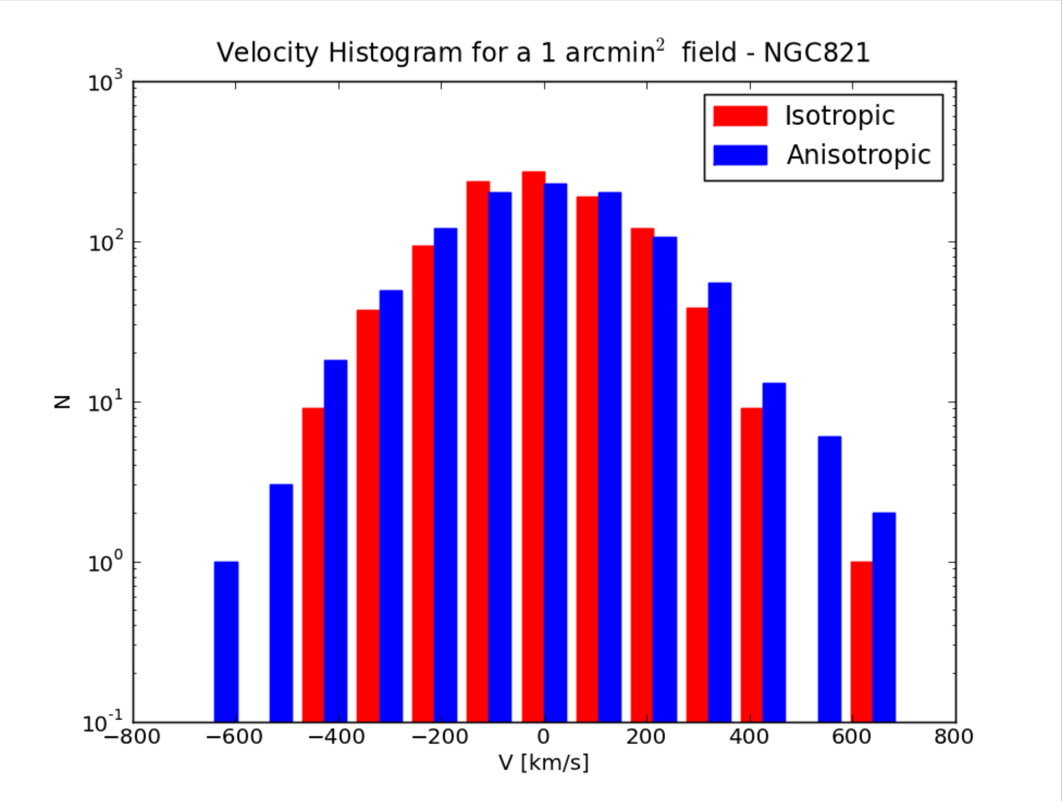

Suppose you work far from the center of NGC 4697

- Then you will sample a small part of the light, therefore the total number of PNs will be small. You would need to detect most of them: you would need to detect extremely faint PNs.
- We need 700; with FOCAS we found 48.
- This is a hard way to go: long exposures in several fields. Unlikely, until we get 30-m or 40-m telescopes.

The situation near the center

- Traditionally rejected as PN searching grounds (very bright background).
- But there is a better way than offband vs onband filters: use the data cube of an integral field spectrograph like MUSE, with its 1 square arc min field, to build monochromatic images at each wavelength. Equivalent to using a very narrow-band filter.
- For example Sarzi et al. 2011 MNRAS 415, 2832 (core of M 32 using SAURON).

PNLF of NGC 4697 from ApJ 563, 135 (2001)

We can predict a total population of about 3500 PNs within 1 arc min of the center.

Given this population, every bin of the PNLF contributes ~30 PNs.

To collect 600 PNs, we need to detect PNs 4 mags fainter than the bright end, which is at

m(5007) = 25.6.

With excellent background subtraction and 0.4 arcsec seeing, it can be done.

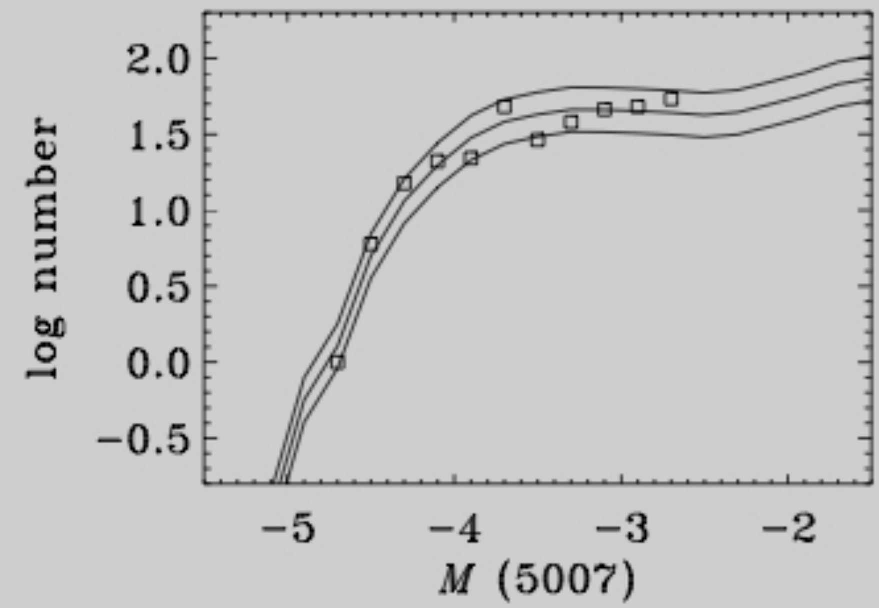

FIG. 14.—Observed [O III] λ5007 PNLF of NGC 4697 (*squares*), with the 328 data binned into 0.2 mag intervals. The apparent magnitudes $m(5007)$ have been transformed into absolute magnitudes $M(5007)$ by adopting an extinction correction of 0.105 mag and a distance modulus $m - M = 30.1$. The three lines are PNLF simulations (Méndez & Soffner 1997) for three different sample sizes: 2500, 3500, and 4900 PNs. From the sample size it is possible to estimate the PN formation rate (see text). The adoption of a distance modulus 29.9 or 30.3 instead of 30.1 would ruin the fit.

Unsolved problems

- PNLF distances are good, but we do not understand why.
- We need to learn more about the PNLF shape (detect fainter PNs). We need deep spectra of the PNs we have discovered (reddening, 5007/Hbeta ratio, abundances).
- PNs are good kinematic tracers. They tell us that intermediate ellipticals are characterized by either a relative lack of dark matter, or substantial radial anisotropy. This ambiguity may be broken by studying PNs at the core of elliptical galaxies like NGC 4697.
- Those same PNs may help to understand the conditions for PN formation in very high metallicity environments, perhaps helping also to better understand the PNLF invariance and shape.

Deep spectra of PNs in NGC 4697

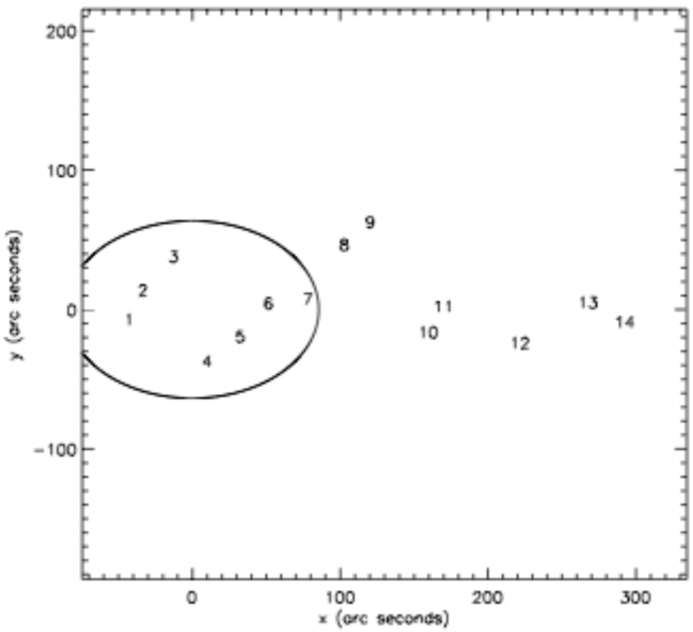

FIG. 4.—Positions of the 14 bright PNs relative to the core of NGC 4697. The area and orientation of this figure are as in Fig. 7 of Méndez et al. (2001). The ellipse is a schematic representation of NGC 4697. The origin of coor-

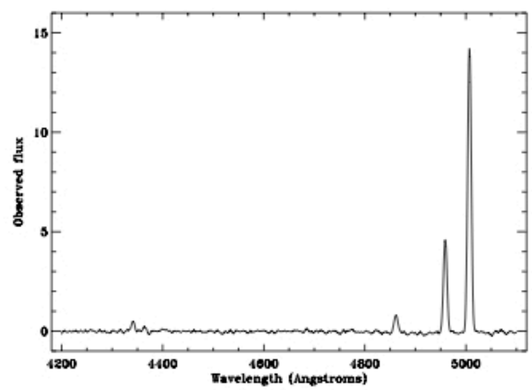

FIG. 9.—Average of all spectra of the 14 PNs in NGC 4697. Visible features are Hγ λ4340, [O III] λ4363, possibly a very weak He II λ4686, Hβ λ4861, and [O III] $\lambda\lambda$4959, 5007.

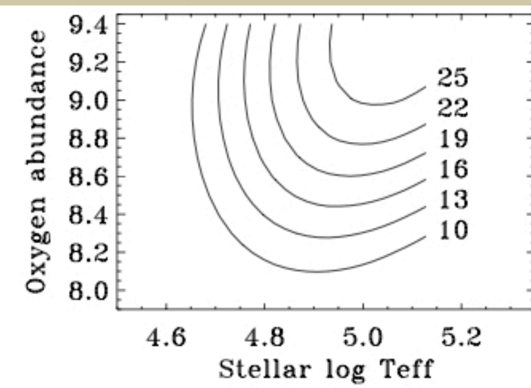

FIG. 11.—Our imitation of Dopita et al.'s (1992) Fig. 3 (see text). Our grid was calculated using CLOUDY. The contours give the λ5007/Hβ ratio as a function of stellar effective temperature (we assume blackbody energy distributions) and oxygen abundance (logarithmic, in the scale where H = 12).

Stop here.